Ignition delay time sensitivity in ignition quality tester (IQT) and its relation to octane sensitivity

Nimal Naser*, S. Mani Sarathy, Suk Ho Chung

King Abdullah University of Science and Technology (KAUST),
Clean Combustion Research Center (CCRC), and,
Physical Science and Engineering Division (PSE). Thuwal, 23955-6900, Saudi Arabia

Abstract

Cetane number (CN) is a commonly used metric to rate the ignition quality of distillate fuels. In this work, a concept of sensitivity in ignition delay time (IDT) obtained with an ignition quality tester (IQT) is proposed, which is correlated to octane sensitivity (OS), i.e., the difference between research octane number (RON) and motor octane number (MON). The concept is based on the determination of IDT using the ASTM D6890 standard and IDT obtained at a temperature lower than that prescribed by the standard. The IDT measured at this lower temperature is referred to as IDT_l, which is obtained via a calibration procedure similar to the ASTM D6890 standard, but with a higher value of reference IDT for calibration with *n*-heptane. The IDT_h (measured at the derived cetane number (DCN) ASTM D6890 condition) of a given test fuel and a binary primary reference fuel (PRF) mixture of *iso*-octane and *n*-heptane was measured to identify a PRF with matching IDT_h as the test fuel. The ratio of low temperature IDTs of the non-PRF test fuel and PRF, i.e., $IDT_{l,non\text{-}PRF}/IDT_{l,PRF}$ was defined as IDT sensitivity (IDS), which was correlated

*Corresponding author
Email address: nimal.naser@kaust.edu.sa (Nimal Naser)

with the OS of the test fuel. The RON and MON values of a wide range of fuel classes including surrogate fuels and fully blended practical fuels were estimated, and showed satisfactory agreement with measured RON/MON values. The RON values of many pure components that could not be measured with standard test methods were also estimated. Two certification diesels and Saudi Arabian pump grade diesel were also tested.
Keywords: octane number, cetane number, autoignition, combustion, ignition delay time, octane sensitivity

1. Introduction

Petroleum-derived and other liquid fuels are dominant global energy resources, accounting for 33% of total energy use in 2012 [1]. Projections in [1] indicate that the share of these liquid fuels could reduce to 30% in 2040, but would still remain an important energy resource. The transport sector, which accounts for 25% of global energy consumption in 2012 [1], is the primary consumer of liquid fuels. The transportation sector utilizes various kinds of liquid fuels depending on the end-use, including gasolines, diesels, jet fuels, biofuels, gas-to-liquids (GTLs), biomass-to-liquids (BTLs), coal-to-liquids (CTLs), etc.

Internal combustion (IC) engines mainly utilize either gasoline or diesel, and mixtures thereof with biofuels and/or alternative fuels. Compression ignition (CI) engines rely on temperature rise due to compression of air to ignite a liquid fuel spray injected into the combustion chamber; and therefore, CI engines require fuels with short ignition delay times (IDTs), such as diesel. CI engine fuels are rated by their cetane numbers (CNs) [2] based on a cetane scale. Recently, derived cetane number (DCN), i.e., CN obtained with an ignition quality tester (IQT) as per the American Society for Testing and Materials (ASTM) D6890 standard [2] is an accepted fuel

rating standard for CI engine fuels.

The cetane scale, or at the time of its introduction known as "cetene" scale was proposed by Boerlage and Broeze [3] in 1932. It assigned a cetene number for a test fuel by matching its ignition quality to diesel primary reference fuels (PRFs) defined for this scale. Initially, the diesel PRFs were cetene (1-hexadecene) and mesitylene (1,3,5-trimethylbenzene) [3]. Cetene being a long chained olefin has high reactivity and easily ignited in a CI engine, while mesitylene being an aromatic has low reactivity making ignition difficult in a CI engine; therefore, cetene and mesitylene were assigned cetene numbers of 100 and 0, respectively. Variations in ignition quality depending on the double bond location of cetene [4] motivated its replacement by cetane (*n*-hexadecane). Subsequently, mesitylene too was replaced by α-methylnaphthalene. This scaling system was adopted by ASTM in 1935 to create the CN, the first standard fuel metric to rate diesel fuels. Due to the expense and difficulty in handling of α-methylnaphthalene; it too was replaced by a highly branched long chain alkane: *iso*-cetane (2,2,4,4,6,8,8-heptamethylnonane) in 1962 [5], which has a reference CN of 15.

The CN of a fuel is measured in a similar manner to the research octane number (RON) and the motor octane number (MON) [6, 7], and are done in accordance with the ASTM D613 standard [8]. The measurements are made in a Cooperative Fuel Research (CFR) F5 engine with diesel PRFs such that the same IDT of a test fuel is obtained with a matching mixture of PRF. As these tests were difficult and time consuming; efforts to determine IDTs with a constant volume combustion chamber (CVCC) progressed [9, 10]. After several efforts, the CVCC developed at Southwest Research Institute [9, 10] was commercialized by Advanced Engine Technology, Ltd. (AET) as the IQT [8, 11–13]. The IQT measures the time delay between the start of injection and appreciable rise in chamber pressure due to ignition. The IDT thus

obtained was correlated to CN obtained with ASTM D613 [8] CFR engine tests. As the CN was not measured in the CFR engine and rather obtained with the CVCC, the measured quantity is referred to as the DCN [2].

Spark ignition (SI) engine fuels are characterized by two standard numbers: RON and MON based on ASTM D2699 and D2700 [6, 7], respectively. The difference between RON and MON is defined as the octane sensitivity (OS). These fuel rating metrics were established in 1927 [14] and are still in use to date without significant changes. A given fuel's RON and MON is determined by following the standard ASTM procedure in an SI CFR F1/F2 engine, and comparing its antiknock quality to that of a mixture of gasoline primary reference fuels (gasoline PRFs): *n*-heptane (RON and MON = 0) and *iso*-octane (2,2,4-trimethylpentane; RON and MON=100). Advances and developments in IC engines from the standard CFR engine condition have shifted presure/temperature history in IC engines such that the fuel standards established in 1927, ASTM D2699 and D2700 [6, 7], may not be able to accurately predict the autoignition characteristics of fuels in modern engines [15–19]. However, these two numbers are able to quantitatively evaluate the changes in autoignition chemistries of gasoline PRFs and gasoline fuels, as explained by Leppard [20]. The negative temperature coefficient (NTC) [21, 22] behavior of PRF mixtures, and the absence of NTC behavior in most practical gasoline fuels [23], results in differences in antiknock quality under RON and MON conditions, which manifests itself as OS [20, 24]. The OS has turned out to be helpful in understanding the influence of fuel chemistry in modern engines, such as in Kalghatgi's concept of octane index (OI) [16, 25]. The OI characterizes a fuel's antiknock quality based on the engine's operating condition (physical characteristic) in addition to the fuel's octane rating

(chemical characteristic). The OI is defined as:

$$OI = (1 - k)RON + kMON \tag{1a}$$

$$OI = RON - k(OS) \tag{1b}$$

When quantifying the OI, the physical characteristic is accounted by k, a linear weighting factor, and the chemical characteristic is accounted by RON and MON. The linear weighting factor, k quantitatively indicates the engine's physical operating condition with respect to the RON and MON conditions. A k value of 1 indicates the engine's pressure/time history is similar to the MON test condition [7] in the CFR engine; in a similar manner, a value of 0 indicates RON test conditions [6]. Studies indicate that operating conditions in modern engines have shifted away from the RON and MON conditions due to changes in engine design and the adoptions of turbocharging and downsizing, i.e., k has reached negative values [17–19, 26]. Thereby fuels with higher RON and lower MON could have better autoignition characteristics in modern engines [26, 27].

Note that in currently developing advanced IC engines, such as low temperature combustion (LTC) engines, autoignition behavior controls operation and an "ideal" fuel may have autoignition behavior in between those of typical gasoline and diesel fuels. Additionally, it is expected that the outlook for transport fuels is to change in the next decades with shift in demand for relatively heavier transport fuels, i.e., diesel and jet fuels [27, 28]. Therefore, it is of vital importance to understand fuel chemistry at conditions apart from a single condition prescribed by ASTM standards [2, 8]. This necessitate the understanding of the relation between octane numbers (ONs) and CNs.

In our recent study in characterizing ignition quality of gasoline fuels [24] in an IQT, it was observed that DCN measurement could satisfactorily predict the RON

of gasoline fuels, while MON could not be predicted. Many studies have correlated CN/DCN with either RON or MON [17, 29–31]. The inability of DCN to correlate both RON and MON could be attributed to the difference in conditions for the RON and MON tests, and the single condition measurement for CN (or DCN) test. In this regard, the present study proposes an additional metric through which the relation between ONs and CNs can also be identified.

The NTC behvior exhibited by PRFs and the absence of NTC behavior for practical gasolines [23] is attributed to OS of practical gasolines as shown in many studies [20, 32–34]. NTC behavior is observed for certain fuels in the IQT [35–38] and other CVCCs [39, 40]. However, the occurence of NTC is a strong function of pressure, equivalence ratio and fuel molecular structure [41–43]. Higher charge pressures in the IQT mitigate NTC behavior [35].

2. Experiments

The experiments were conducted in a KAUST research-ignition quality tester (KR-IQT) obtained from AET. The device was equipped with a variable displacement pump (VDP), a modification to the standard IQT, the latter that is available elsewhere. Using this equipment, a methodology has been developed in relating octane numbers to IDTs measured in an IQT in [24] by maintaining a global equivalence ratio (ϕ_{global}) that is fixed among tested fuels.

The standard IQT has a fixed displacement pump (FDP), thereby the volume of fuel injected is fixed that results in changes in the mass of fuel injected based on the density of fuel. This change in mass of fuel injected results in changes in ϕ_{global}. In spite of the differences in ϕ_{global} among tested fuels, the ASTM D6890 standard for DCN measurement prescribes a fixed volume of fuel injected. This motivated us in developing a methodology to relate IDTs measured in a standard IQT, i.e., IQT

equipped with an FDP. Thus, the approach put forward in this paper is suitable to any standard IQT. The IDTs reported in this work were determined based on the gradient method [24, 44] to account for heat release due to low temperature reactions. More details on the gradient method, the motivation for using the gradient method and experimental setup are available in [24, 44].

As the IQT relies on liquid fuel injection, the measured IDT depends on many physical factors, particularly the physical properties of fuel, and thermal and mixture inhomogeneities. The effects of thermal and mixture inhomogeneities are difficult to quantify experimentally due to the lack of optical access for the IQT for imaging techniques; however, efforts in this direction were carried out computationally by Bogin et al. [35, 45], and Osecky et al. [37]. These studies concluded that for short IDTs, the fuel-air mixture is heterogeneous; for long IDTs a quasi-homogeneous region exists in the IQT. However, in spite of mixture heterogeneity for short IDTs, consistent IDTs are obtained for 32 injections for one particular fuel with negligible standard deviation in the results.

The physical properties of fuel influence spray physics and thereby the physical delay times [35–37, 45, 46]. However, the physical delay times for gasoline-like fuels are negligibly small compared with the long IDTs, as shown experimentally in [47] and computationally in [35–37, 46]. The IDTs obtained with an IQT were separated into physical and chemical delay times with second derivative inflection point analysis (ddP method) and minimum change in pressure integration of the IQT pressure signal by Mendelson [47]. It was shown experimentally that for less reactive fuels chemical delay times dominated physical delay times, and for more reactive fuels the physical delay times could dominate chemical delay times, but their study was able to prove that physical delay times are consistent among fuels. Similar observations showing that ignition processes in less reactive fuels are governed by chemical kinetics were

computationally made in [35–37, 46].

Tables S1 to S4 lists the details of the fuels measured in the present study. Compositional details of gasoline PRFs for octane tests [6, 7], toluene reference fuels (TRFs) and toluene primary reference fuels (TPRFs) are given in Table S1. PRFs are binary mixtures of *iso*-octane and *n*-heptane, standard reference fuels that define the octane scale [6, 7]. A PRF X indicates X vol% of *iso*-octane and remaining *n*-heptane; the vol% of *iso*-octane being the RON/MON of the PRF mixture. TRFs are binary mixtures of toluene and *n*-heptane, that were defined to impart sensitivity to replicate practical gasoline behavior [48, 49]. A TRF X indicates X vol% of toluene and remaining *n*-heptane. However, as TRFs were able to satisfy either RON or MON only, an additional component to these binary mixtures enabled the mixtures to satisfy RON and MON together which led to definitions of TPRFs [50, 51]. These are ternary mixtures of toluene, *iso*-octane, and *n*-heptane. A TPRF X-Y indicates X vol% of toluene, Y vol% of *iso*-octane and remaining *n*-heptane.

Unlike gasoline PRFs, the RON/MON of TRFs and TPRFs have to be estimated from empirical blending rules developed with detailed experimental engine measurements as given in [51]. Recently, the RON and the MON of various multicomponent surrogate blends (MCSBs) with similar RON but different OSs were measured in [52, 53]. Gasoline surrogates of varying OS at set values of RON were obtained in [52] with surrogate component fuels of *n*-heptane, *iso*-octane, toluene, ethanol and *iso*-butanol. In [53] surrogate mixtures with similar RON and differing OSs were achieved by using various components in addition to toluene, such as 1-hexene, cyclopentane (CPT) and 1,2,4-trimethylbenzene (124-TMB) [54]. However, the mixtures in [52] were not tested as part of this work as the MON values in [52] are predicted, with only RON values obtained with standard ASTM D2699 tests. Therefore, mixtures in [53] were tested as part of this work as both RON and

MON values were obtained with ASTM D2699 and D2700 tests [6, 7], respectively. The compositional details and RON/MON of various MCSBs in [53] are given in Table S2. In addition to surrogates, it was also important to measure practical gasolines with the renewed interest in understanding interaction of fuel and engine design from a fundamental perspective. To this end, fully blended gasolines, fuels for advanced combustion engines (FACE) gasolines [55], certification gasolines, and FACE gasolines blended with ethanol were also studied in the present work as given in Tables S3 and S4.

The IDTs of all the mixtures were measured at the standard DCN condition [2], which requires the IDT of the fuel to be measured in zero air (air containing trace amount of hydrocarbons) at a charge pressure (P_0) of 21.37 $\pm$ 0.07 bar and a standard temperature fixed by a calibration procedure. The standard temperature was obtained by adjusting the temperature such that the average of three n-heptane runs has an IDT of 3.78 $\pm$ 0.01 ms. Each run involves 15 pre-injections to create a stable operating environment for the succeeding 32 main injections; the average of these 32 injections are reported in the present work and referred to as $\mathrm{IDT_h}$. In a similar manner, IDT measurements were obtained at a lower temperature following a similar calibration procedure, but instead of 3.78 ms; the temperature is fixed by the average of three n-heptane runs that has an IDT of 7.56 $\pm$ 0.04 ms. The IDT measured at the lower temperature is referred to as $\mathrm{IDT_l}$ and the condition is referred to as the low temperature IQT condition. This IDT value of 7.56 ms was chosen arbitrarily to be the double that was measured at the standard DCN temperature.

In the present work, the high temperature measurements were obtained at 835–845 K and the low temperature measurements at 755–765 K. An IDT at an intermediate temperature of 800 K was also obtained to confirm the trends in IDT variation with temperature, but were not used in analysis. The DCN was calculated

from the measured IDT_h using Eq. (2) as prescribed by ASTM D6890 [2]. The equations are defined depending on the range of the measured IDT_h; for IDT_h in the range of 3.1 to 6.5 ms Eq. (2a) is used, for IDT_h outside the range Eq. (2b) is to be used. Note that the IQT was designed to characterize diesel like fuels, i.e., fuels with DCN in the range of 40–60. As a result, extensive tests [13, 56] in this range have led to the development of precise correlation as given by Eq. (2a); however, the correlation given by Eq. (2b) is less precise. In spite of this, many recent publications [30, 57–60] have employed correlation Eq. (2b) to obtain DCN of fuels whose IDT lie outside the range of 3.1–6.5 ms.

$$DCN = 4.46 + \frac{186.6}{\tau_{id}[\text{ms}]} \tag{2a}$$

$$DCN = 83.99\left[(\tau_{id}[\text{ms}] - 1.512)^{-0.658}\right] + 3.547 \tag{2b}$$

3. Ignition delay time sensitivity concept

Fuel autoignition chemistry has a strong dependence on the pressure/time history of the engine. The push to increase IC engine efficiency, and more importantly, lower engine-out emissions has initiated research into new engine combustion concepts [61–63]. The right fuel for these concept engines is still an open research question, and necessitates further understanding of fuel's ignition quality at various operating conditions. This paper introduces the concept of IDT sensitivity (IDS) , to account for the sensitivity of IDT with temperature changes.

Figure 1 shows the measured IDTs of fuels with similar RON but different OS by varying initial temperature T_0. The result shows that for the gasoline PRFs (PRF 80, 83 and 90 in Fig. 1(a), and PRF 90 and 100 in Fig. 1(b)), they show a reasonably

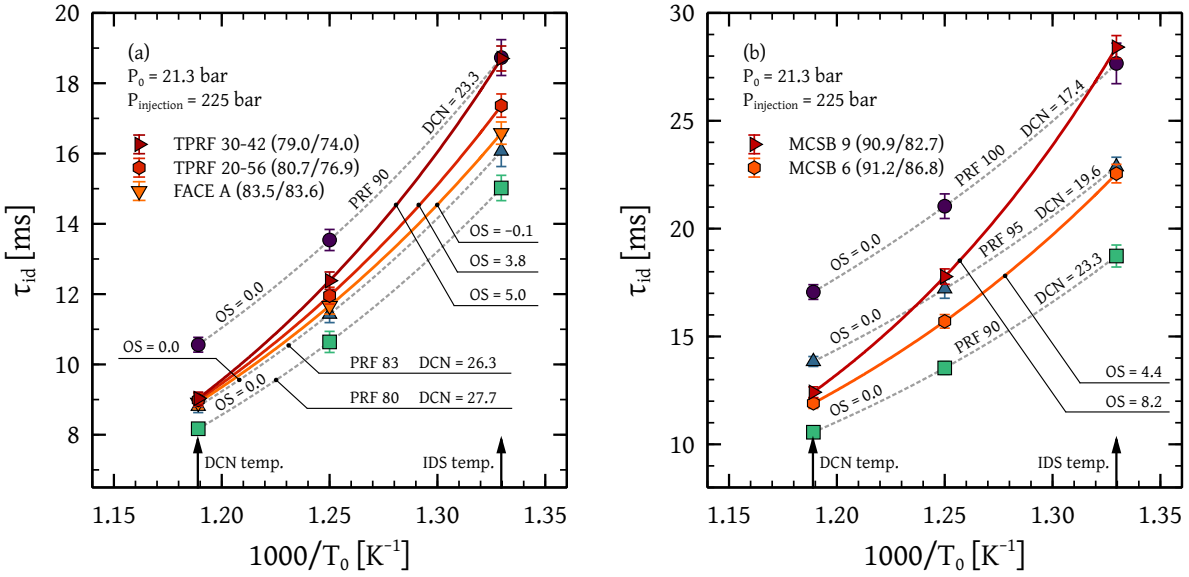

Figure 1: IDTs measured in IQT of fuels with similar RON but different OSs. Values in parantheses indicate RON and MON, respectively. ((a)) RON∼83 ((b)) RON∼91.

parallel behavior when plotted IDTs with ${T_0}^{-1}$. While the fuels having the same DCN measured at the standard condition ($1000/T_0 = 1.1891$ K^{-1} or 841 K) behave differently as T_0 changes from the standard condition. Compositional details of PRFs and TRFs are available in the Supplementary Material (Table S1). Figure 1(a) shows the IDTs of three PRFs (OS = 0), along with TPRFs of varying OS. Also shown are the measured IDTs of a fully blended gasoline: FACE A gasoline. Note that PRF 80, TPRF 30-42, TPRF 20-56 and FACE A gasoline have similar RON($\approx$ 79.0–83.5) but have different OSs. FACE A gasoline has the smallest OS ($= -0.1$) and has an IDT behaving similar to PRF 83 as T_0 varies. In TPRFs, increasing toluene concentration increases OS of the TPRF mixture [50, 51, 53, 54]. As observed in Fig. 1(a), the fuels with similar RON but different OS have similar IDT at the DCN condition, but exhibits different IDT behavior at the low temperature IQT condition as compared

with PRFs. Therefore, for a non-PRF such as TPRF 30-42, it can be observed that at the low temperature IQT condition, it has IDT similar to PRF 90, i.e., its autoignition quality has improved and thereby does not behave like a PRF.

The differences in IDTs between sensitive and non-sensitive fuels have important implication on fuel engine design because autoignition in IC engines evolves over a wide range of pressure and temperature, in contrast to single pressure and temperature conditions in a CVCC (e.g., an IQT). However, understanding the differences in fuel behavior in a standard device such as IQT may provide better insights into how fuels behave in engines; thus motivating the present work.

The IDS of a non-PRF is defined as the ratio of IDT measured at the low temperature IQT condition (i.e., IDT_l) of the non-PRF and PRF, when the non-PRF and PRF have matching DCN or IDT_h. IDS is defined as a ratio instead of a difference as the latter provided a decorrelation with OS. Hence, IDS was defined as the ratio of IDT_l of the non-PRF and PRF. More details on will be discussed later. As mentioned above, the IDT_h is measured at the standard conditions defined in ASTM D6890 [2], and IDT_l is measured at a lower temperature, while maintaining the same pressure and volume of fuel injected (to be aligned with standard IQTs available elsewhere). Note that varying temperature while maintaining pressure and volume of fuels results changing ϕ_{global}. The IDT_l at non-standard conditions was evaluated at a lower temperature due to (1) limitations of the IQT in measuring IDTs at temperatures greater than 873 K, where IDT could be correlated with MON as shown in [24] and (2) the need for understanding low temperature ignition behavior in advanced IC engines. IDS is then defined as:

$$IDS = \frac{IDT_{l,non-PRF}}{IDT_{l,PRF}} \quad \Leftrightarrow \quad DCN_{non\text{-}PRF} \approx DCN_{PRF} \tag{3}$$

The IDTs at DCN and IDS conditions are given in Table S5 in Supplementary

Material.

The IDT_l is always higher than IDT_h as the latter is evaluated at higher temperatures. This was also true for fuels that typically display NTC behavior. The IDS for a fuel with zero OS, such as a PRF, is different from a fuel with OS > 0. The difference in IDS for fuels with varying OS can be better explained with Fig. 1, which shows IDTs of PRFs 80, 83, and 90, and three fuels with varying OS. The latter fuels have almost similar RON but different MON. It can be observed that as the fuel's OS increases, the IDTs at lower temperatures (i.e., IDT_l) deviate more from the IDT of the PRF with matching IDT measured at the DCN condition. For example, it can be observed that fuels with OS > 0 have IDT at lower temperatures that approaches that of a higher PRF than that was matched at the DCN condition. This is due to negative k values for the present conditions in the IQT, as was shown in [24].

The IDT_l of PRFs follows a nonlinear trend with the IDT_h, as shown in Fig. 2. The variation of IDT_l of PRF with IDT_h can be fitted to a nonlinear function as given in Eq. (4). The IDT_l of PRFs up to PRF 100 ($IDT_l \approx 28$ms) are shown in Fig. 2. Due to the unavailability of zero OS fuels with RON greater than 100, the IDT_l of fuels with zero OS were estimated by analyzing the variation in IDT_l of PRFs. The variation of IDT_h and IDT_l is shown in Fig. S1. The IDT_l is observed to have a piecewise linear behavior as seen in Fig. S1. The nonlinear regression model for higher PRFs was used to estimate the IDT_l for PRFs with RON > 100, i.e., zero OS fuels with RON > 100. The IDT_l thus obtained is shown in inset of Fig. 2. The nonlinear regression model given by Eq. (4) will be used to estimate the mboxIDT$_l$ of PRF with matching DCN or IDT_h as the non-PRF; in order to quantify the relationship between OS and IDS. Note that Eq. (4) is valid only for PRFs, while the IDS of non-PRF can be determined by Eq. (3).

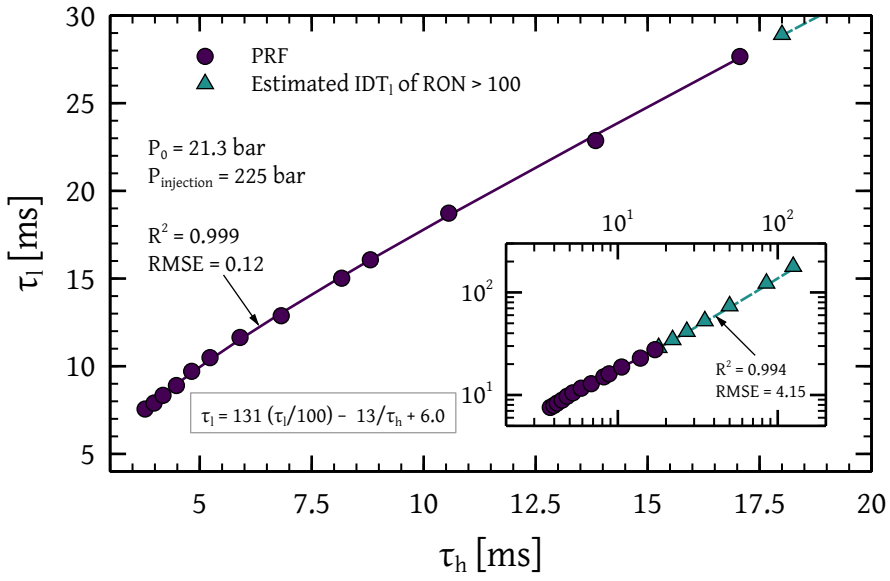

Figure 2: Variation of IDT_l with IDT_h of various PRFs

$$\tau_{l,PRF} = 131\left(\frac{\tau_h}{100}\right) - \left(\frac{13}{\tau_h}\right) + 6.0 \tag{4}$$

A comparison of the fuel's IDS with its corresponding OS is shown in Fig. 3. As observed in Fig. 3, the IDS exhibits a correlation with OS. A logarithmic correlation with coefficient of determination $R^2 = 0.788$ given by Eq. (5) can be utilized to estimate the OS of a fuel for a given IDS. An IDS = 1 indicates that the IDT_l of non-PRF is same as the IDT_l of PRF and thereby indicates the OS of the non-PRF is 0.

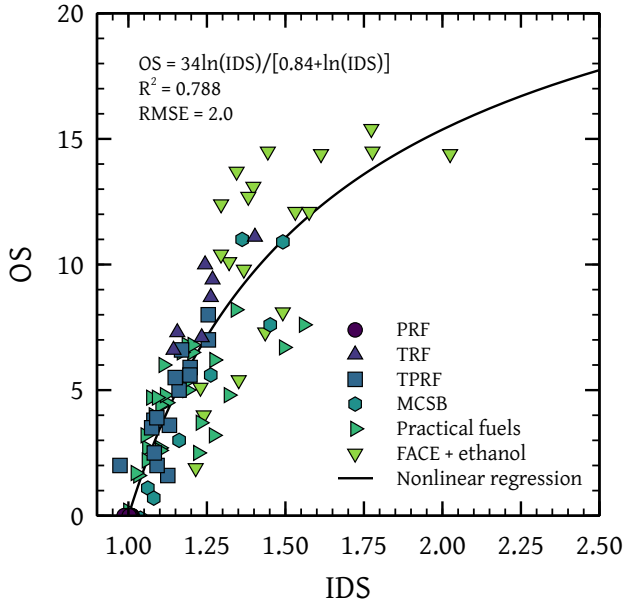

Figure 3: Correlation of OS with IDS

$$OS = \frac{34ln(IDS)}{[0.84 + ln(IDS)]} \tag{5}$$

As an example, consider the IDT of MCSB 9 and 20 as shown in Fig. 4 at the DCN and low temperature IQT conditions, details on the composition of MCSBs are available in Table S2. The RON/MON/DCN of MCSB 9 is 90.9/82.7/21.0 and as explained above, a single DCN was not able to predict fuel reactivity at other temperatures (lower temperature in this case). The measured IDT_h and IDT_l of MCSB 9 was 12.4 and 28.4 ms, respectively; for this IDT_h value, the IDT_l of PRF is estimated to be 21.2 ms (using Eq. (4)). The IDS of MCSB 9 calculated with Eq. (3) is 1.34, which on substitution in Eq. (5) provides an OS of 8.8. The predicted OS is very close to the measured OS = 8.2 [53]. In a similar manner the OS of MCSB 20 is predicted to be -0.1 compared to measured OS = 0.2 [53]. However, some errors in the prediction of OS were observed. The highest error in the prediction was

observed for FACE F gasoline blended with 25 vol% of ethanol; the predicted OS was 8.9 compared to the measured OS = 13.7. Compared to the ASTM tests the predictions are less accurate; however, the present methodology can be a rapid tool in fuel screening which may not be feasible in cetain cases using a CFR engine, and when fuel sample quantities are available in limited quantites and/or have low vapor pressures.

It was demonstrated in [24], that a potential correlation exists between the RON and DCN in the form given by (6), which was used to estimate RON referred to as $\text{RON}_{\text{predicted}}$ in the present study. With the estimated RON and the OS, the MON of the mixture was evaluated as MON = RON − OS. Applying the above methodology to the mixtures given in Tables S1 to S4; the RON and MON were estimated as given in Table S5, the comparisons of which are provided in the next section.

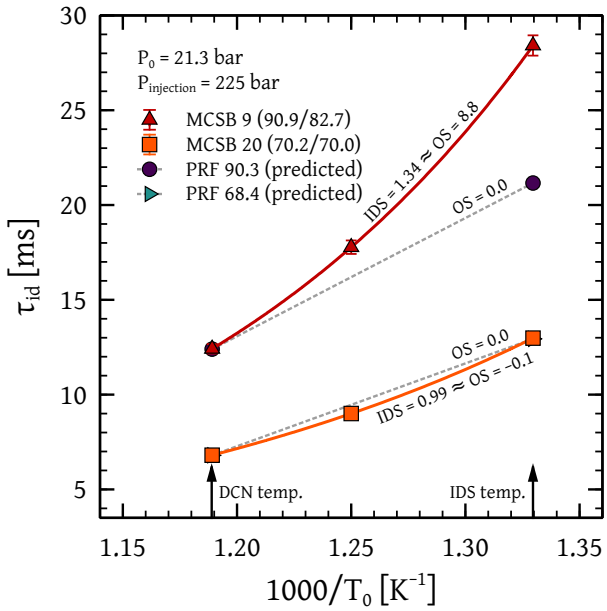

Figure 4: IDS of various MCSBs

$$RON_{predicted} = -293\left(\frac{DCN}{100}\right)^2 - 52\left(\frac{DCN}{100}\right) + 114.1 \quad (6)$$

4. Ignition delay time sensitivity applied to surrogate and practical fuels

4.1. Comparison of estimated and nominal RON

The estimated RON with the correlation Eq. (6) obtained in [24] was compared with nominal RON available in literature. The comparisons are shown in Fig. 5 with values given in Table S5. The predictions were excellent indicated by the high R^2 (= 0.980) and low root mean square error (RMSE) (= 2.7) for the various mixtures tested in the present study. The maximum error (ϵ_{max}) was observed to be 7.1 indicated by the red circle in Fig. 5, this is comparatively higher than the $\pm$0.7 reproducibility error associated with the RON tests [6]. However, the reproducibility error of $\pm$0.7 is associated with experimental measurements alone, while the comparisons made here are between a model-based approach and experimental measurements, in which case an error of 7.1 may be acceptable for the applications such as initial fuel screening, surrogate fuels development, assessing the viability of fuel additives as octane boosters, etc.

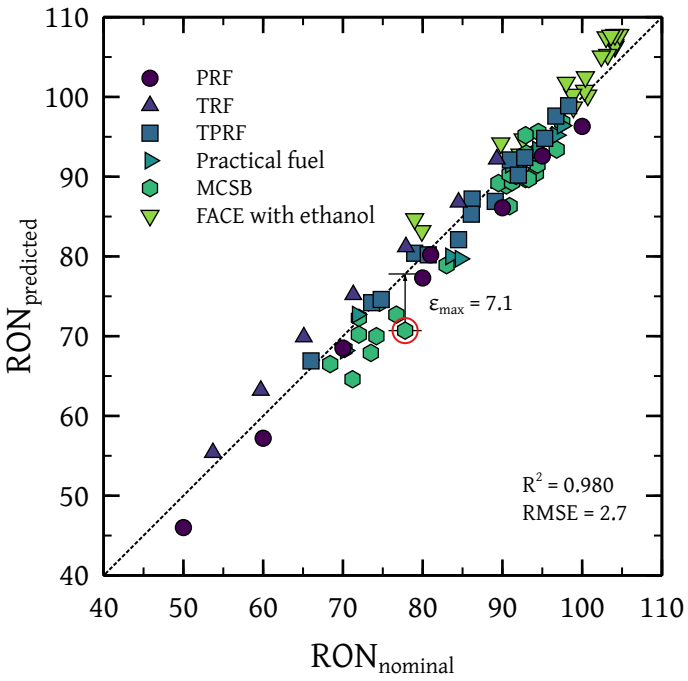

Figure 5: Comparison of estimated and nominal RON

4.2. Comparison of estimated and nominal MON

With the concept of IDS, OS of various fuels measured in the present study is estimated to determine the fuel's MON. The IDT_h of the non-PRF obtained at the DCN condition is used to determine IDT_l of the PRF with Eq. (4); together with the IDT_l of the non-PRF obtained at the low temperature IQT condition the IDS is obtained with Eq. (3). The OS is then esimated with the resulting IDS using Eq. (5) as given in Table S5. As the OS is the difference between RON and MON, the MON is estimated with RON and OS, and RON being estimated with Eq. (6). The estimated MON had reasonable agreement with the nominal MON indicated by the high R^2 (= 0.961) and low RMSE (= 3.5) as shown in Fig. 6. For MON estimations, ϵ_{max} = 8.0 indicated by the red circle, this is also higher than the ±0.9 reproducibility error associated with the MON tests [7]. Despite this difference, the

method is fairly good in estimating the MON of fuels that cannot be measured with the conventional method [7].

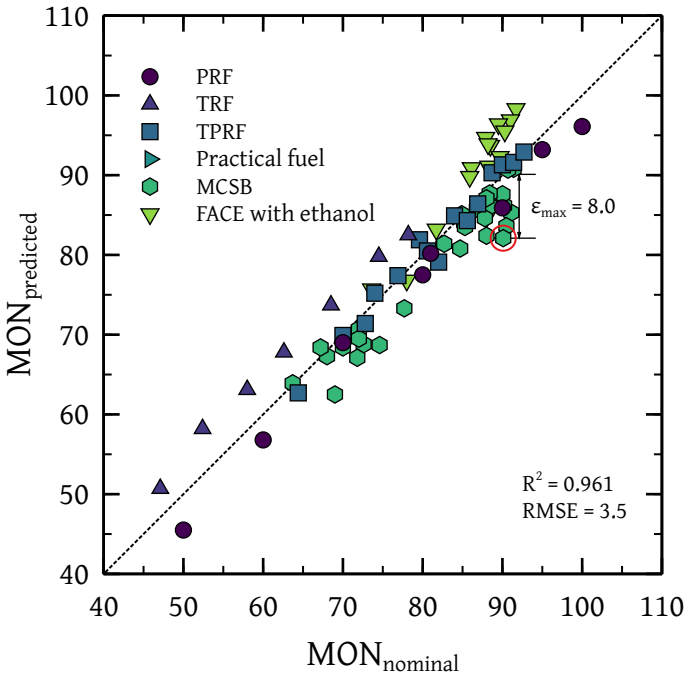

Figure 6: Comparison of estimated and nominal MON

4.3. Comparison of estimated and nominal RON with DCN obtained from literature

The validity of the method were also tested by comparing RON estimated with DCN obtained from literature to nominal RON values as given in Table S6. In some cases, one compound had two different values of DCN as multiple literature sources were available for them, in such cases the closest matching case is given in Table S6 and other values are given in Table S7 in Supplementary Material. Comparisons of predicted RON and nominal RON of all fuel mixtures in Table S6 are given in Fig. 7

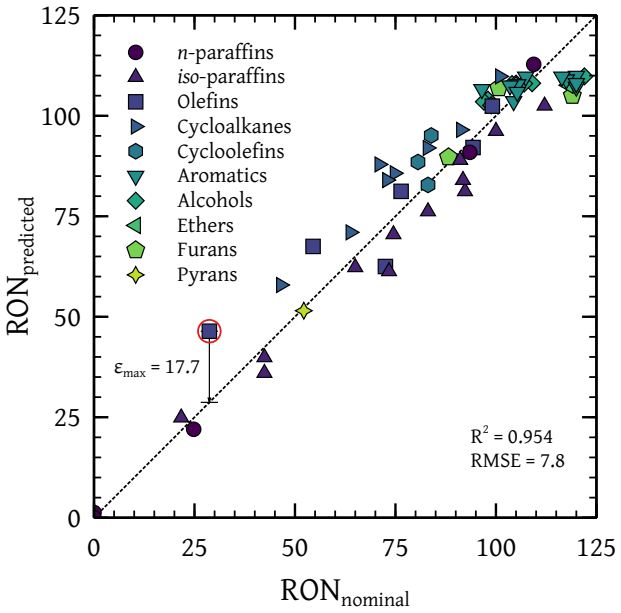

Figure 7: Comparison of estimated and nominal RON of various hydrocarbons given in Table S6

Comparisons between estimated RON and nominal RON for different classes of chemicals are shown in Fig. 7. For very high RON (>100) and low RON (<40) the predictions were poor, as measurement of RON > 100 is not well defined by ASTM D2699 [6] and is subject to greater uncertainties as reproducibility limits keep increasing for RON > 100 [6]. It is interesting to note the RON standard ASTM D2699 is defined to measure RON > 40 in spite of this the literature has many RON measurements below 40. Taking into effect these limitations, the predictions have $R^2 = 0.954$ and RMSE = 7.8, comparatively poorer than predictions made in § 4.1 (Fig. 5). In estimating RON, $\epsilon_{max} = 17.7$ was observed for RON < 40, indicated by the red circle in Fig. 7.

Due to limitations in measuring RON of low vapor pressure fuels, the RON of many fuels are not available in literature. However, their DCN is readily available as an IQT is designed to characterize such fuels. Hence, a rough estimation of their

RON is made in Table S8 using the correlation given by Eq. 6. It is to be noted that the RON values reported in Table S8 are estimated and not measured, and any such measurements would be helpful in validating the correlations proposed.

As the DCNs available in literature are measurements made at the ASTM D6890 [2] condition only, IDT_l values at low temperature IQT conditions are not available; and hence for the fuels given in Table S6 the MON cannot be estimated. However, many of the compounds are components of novel biofuels, and many others are potential octane boosters. The evaluation of their autoignition characteristics at lower temperatures would be highly beneficial to fuel designers and the combustion community.

4.4. Ignition delay time sensitivity of diesel fuels

The predictions made so far involved gasoline and gasoline-like fuels. With the shift in fuel demand to diesel and jet fuels [28], and increasing interest in biodiesels [64–67], it was imperative to determine the IDS of diesels. To this end, the IDS of two certification diesels: (1) Coryton US2D diesel and (2) Coryton Euro diesel without FAME, and practical diesel: Saudi Arabia (SA) pump grade diesel was determined.

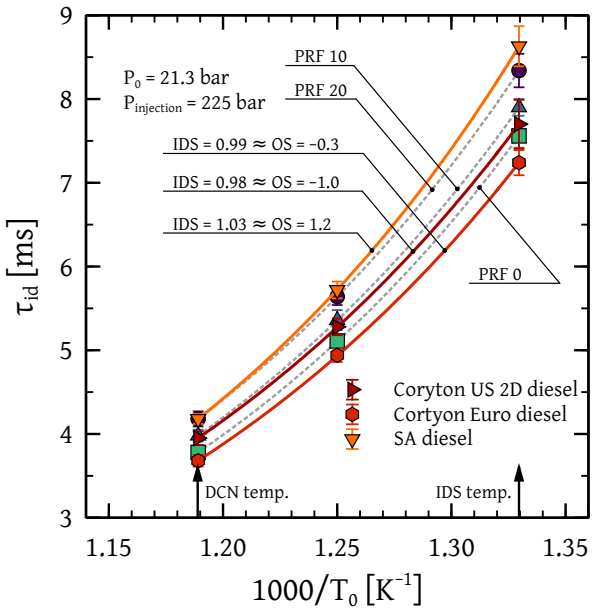

Figure 8: IDS of Coryton and SA pump grade diesels with PRF 0 for comparison

The IDTs of various diesels were measured at both DCN and the low temperature IQT condition as shown in Fig. 8. It can be observed that the IDT curves of both Coryton and SA diesels have identical slopes as that of PRFs 0, 10 and 20 at both DCN and low temperature IQT conditions. The IDS calculated for both diesels have values close to or lesser than 1 indicating they have negligible to nil OS. From the observations made above it can be inferred that the behavior of diesels are similar to PRFs (i.e., *n*-heptane); making *n*-heptane ideal as a chemical kinetics surrogate for diesel as demonstrated in [44, 68, 69]. This can be understood as diesels are primarly composed of long carbon chain length (typically 10–22) *n*-paraffins and *iso*-paraffins [70], which have notable NTC [21, 22] behavior. Although diesel has appreciable amount of aromatics, and most of the aromatics are alkyl substituted aromatics with long chain alky groups [68, 70]. These long chain alkyl groups mask the presence of attached aromatic ring and with the former as the reactivity

determining groups due to their long chain lengths explains the low IDS or OS of diesels.

5. Concluding remarks

The difference in IDT of a fuel in an IQT was utilized in defining IDS, a new concept to quantify the sensitivity of the fuel's ignition quality with temperature. The IDS of a fuel was defined as the ratio of the IDT_l of the test fuel and a PRF such that the test fuel and PRF have matching DCN or IDT_h. The IDS condition has a temperature lower than the standard DCN temperature. The IDT_l for various PRFs were measured and a nonlinear variation with IDT_h was obtained. This nonlinear regression model for IDT_h of PRFs with IDT_l at IDS condition is also reported. The ratio of the IDT_l of the non-PRF and PRF with matching IDT_h of the non-PRF as described above was observed to correlate with OS of the non-PRF. The logarithmic correlation of the IDS of the non-PRF with OS enabled estimation of the OS of any unknown fuel/mixture by IDT measurements at two well-defined conditions: DCN and IDS.

The RON of fuels/mixtures tested with the KR-IQT in the present work were estimated with a previously established correlation and showed good agreement with nominal RON. The OS estimated from the IDS is utilized in predicting the MON of the fuels/mixtures and shows reasonable agreement with nominal MON. The RON of other compounds whose DCN and nominal RON were available in the literature were also compared showing substantial degree of accuracy in predictions. For some compounds DCN values were available but their RON could not be measured for various reasons, for such compounds the RON were also estimated in the present work. Although these values are not the actual RON, it is helpful in estimating the approximate range of their anti-knock quality. Future RON measurements of

these compounds (of unknown RON) would be beneficial in validating the proposed correlations. Finally, the IDS and OS of two certification diesels and one practical diesel were measured and the IDSs were comparable to PRFs due to the presence of long chain *n*-paraffins, *iso*-paraffins and long chain alkyl substituted aromatics. From the observations made for diesel fuels, it can be concluded that IDS can be treated as the cetane sensitivity corresponding to OS for diesel fuels.

Acknowledgments

The research reported in this paper was funded by Saudi Aramco and the Clean Combustion Research Center at King Abdullah University of Science and Technology under the FUELCOM program.

References

[1] Energy Information Administration, International energy outlook 2016, Tech. rep. (2016).
URL https://www.eia.gov/outlooks/ieo/pdf/0484(2016).pdf

[2] ASTM D6890, Standard test method for determination of ignition delay and derived cetane number DCN of diesel fuel oils by combustion in a constant volume chamber, ASTM International.doi:10.1520/D6890-15B.

[3] G. Boerlage, J. Broeze, Ignition quality of diesel fuels as expressed in cetene numbers, SAE technical paper 320007 (1932). doi:10.4271/320007.

[4] J. Van Gerpen, Cetane number testing of biodiesel, in: Proceedings of the third liquid fuels conference, 1996, pp. 197–206.

[5] G. E. Totten, S. R. Westbrook, R. J. Shah, Fuels and lubricants handbook, ASTM International (01-June-2003)doi:10.1520/MNL37-EB.

[6] ASTM D2699-13b, Standard test method for research octane number of spark-ignition engine fuel, ASTM International.doi:10.1520/D2699.

[7] ASTM D2700, Standard test method for motor octane number of spark-ignition engine fuel, ASTM International.doi:10.1520/D2700-16.

[8] ASTM D613, Standard test method for cetane number of diesel fuel oil, ASTM International.doi:10.1520/D0613-16A.

[9] T. W. Ryan, Correlation of physical and chemical ignition delay to cetane number, SAE technical paper 852103 (1985). doi:10.4271/852103.

[10] T. W. Ryan, T. J. Callahan, Engine and constant volume bomb studies of diesel ignition and combustion, SAE technical paper 881626 (1988). doi:10.4271/881626.

[11] L. N. Allard, G. D. Webster, N. J. Hole, T. W. Ryan, D. Ott, C. W. Fairbridge, Diesel fuel ignition quality as determined in the ignition quality tester (IQT), SAE technical paper 961182 (1996). doi:10.4271/961182.

[12] L. N. Allard, N. J. Hole, G. D. Webster, T. W. Ryan, D. Ott, A. Beregszazy, C. W. Fairbridge, J. Cooley, K. Mitchell, E. K. Richardson, N. G. Elliot, D. J. Rickeard, Diesel fuel ignition quality as determined in the ignition quality tester (IQT)- Part II, SAE technical paper 971636 (1997). doi:10.4271/971636.

[13] L. N. Allard, G. D. Webster, T. W. Ryan, G. Baker, A. Beregszaszy, C. W. Fairbridge, A. Ecker, J. Rath, Analysis of the ignition behaviour of the ASTM D-613 primary reference fuels and full boiling range diesel fuels in the ignition quality tester (IQT^{TM}) - Part III, SAE technical paper 1999-01-3591 (1999). doi:10.4271/1999-01-3591.

[14] G. Edgar, Measurement of knock characteristics of gasoline in terms of a standard fuel, Industrial & Engineering Chemistry 19 (1) (1927) 145–146. doi:10.1021/ie50205a049.

[15] G. Kalghatgi, Fuel/engine interactions, SAE Internationaldoi:10.4271/R-409.

[16] G. T. Kalghatgi, Fuel anti-knock quality - Part I. Engine studies, SAE Technical Paper 2001-01-3584 (2001). doi:10.4271/2001-01-3584.

[17] G. T. Kalghatgi, Auto-ignition quality of practical fuels and implications for fuel requirements of future SI and HCCI engines, SAE Technical Paper 2005-01-0239 (2005). doi:10.4271/2005-01-0239.

[18] V. Mittal, J. B. Heywood, The relevance of fuel RON and MON to knock onset in modern SI engines, SAE Technical Paper 2008-01-2414 (2008). doi:10.4271/2008-01-2414.

[19] V. Mittal, J. B. Heywood, The shift in relevance of fuel RON and MON to knock onset in modern SI engines over the last 70 years, SAE International Journal of Engines 2 (2009-01-2622) (2009) 1–10. doi:10.4271/2009-01-2622.

[20] W. R. Leppard, The chemical origin of fuel octane sensitivity, SAE Technical paper 902137 (1990). doi:10.4271/902137.

[21] J. Griffiths, Negative temperature-coefficient of reaction rate during hydrocarbon oxidation, Journal of the Chemical Society D: Chemical Communications (9) (1969) 483b–484. doi:10.1039/C2969000483B.

[22] I. A. Leenson, G. B. Sergeev, Negative temperature coefficient in chemical reactions, Russian Chemical Reviews 53 (5) (1984) 417–434. doi:10.1070/RC1984v053n05ABEH003060.

[23] S. M. Sarathy, A. Farooq, G. T. Kalghatgi, Recent progress in gasoline surrogate fuels, Progress in Energy and Combustion Science 65 (2017) 67–108. doi:10.1016/j.pecs.2017.09.004.

[24] N. Naser, S. Y. Yang, G. Kalghatgi, S. H. Chung, Relating the octane numbers

of fuels to ignition delay times measured in an ignition quality tester (IQT), Fuel 187 (2017) 117–127. doi:10.1016/j.fuel.2016.09.013.

[25] G. T. Kalghatgi, Fuel anti-knock quality - Part II. Vehicle studies-how relevant is motor octane number (MON) in modern engines?, SAE Technical Paper 2001-01-3585 (2001). doi:10.4271/2001-01-3585.

[26] G. T. Kalghatgi, K. Nakata, K. Mogi, Octane appetite studies in direct injection spark ignition DISI engines, SAE Technical Paper 2005-01-0244 (2005). doi:10.4271/2005-01-0244.

[27] G. Kalghatgi, Developments in internal combustion engines and implications for combustion science and future transport fuels, Proceedings of the Combustion Institute 35 (1) (2015) 101–115. doi:10.1016/j.proci.2014.10.002.

[28] G. T. Kalghatgi, The outlook for fuels for internal combustion engines, International Journal of Engine Research 15 (4) (2014) 383–398. doi:10.1177/1468087414526189.

[29] T. W. Ryan, A. C. Matheaus, Fuel requirements for HCCI engine operation, SAE Technical Paper 2003-01-1813 (2003). doi:10.4271/2003-01-1813.

[30] P. L. Perez, A. L. Boehman, Experimental investigation of the autoignition behavior of surrogate gasoline fuels in a constant-volume combustion bomb apparatus and its relevance to HCCI combustion, Energy and Fuels 26 (10) (2012) 6106–6117. doi:10.1021/ef300503b.

[31] R. L. McCormick, G. Fioroni, L. Fouts, E. Christensen, J. Yanowitz, E. Polikarpov, K. Albrecht, D. J. Gaspar, J. Gladden, A. George, Selection

criteria and screening of potential biomass-derived streams as fuel blendstocks for advanced spark-ignition engines, SAE International Journal of Fuels and Lubricants 10 (2017-01-0868) (2017) 442–460. doi:10.4271/2017-01-0868.

[32] M. Mehl, T. Faravelli, F. Giavazzi, E. Ranzi, P. Scorletti, A. Tardani, D. Terna, Detailed chemistry promotes understanding of octane numbers and gasoline sensitivity, Energy & fuels 20 (6) (2006) 2391–2398. doi:10.1021/ef060339s.

[33] M. Mehl, J.-Y. Chen, W. J. Pitz, S. M. Sarathy, C. K. Westbrook, An approach for formulating surrogates for gasoline with application toward a reduced surrogate mechanism for CFD engine modeling, Energy & Fuels 25 (11) (2011) 5215–5223. doi:10.1021/ef201099y.

[34] N. Naser, S. M. Sarathy, S. H. Chung, Estimating fuel octane numbers from homogeneous gas-phase ignition delay times, Combustion and Flame 188 (2018) 307–323. doi:10.1016/j.combustflame.2017.09.037.

[35] G. E. Bogin Jr, E. Osecky, M. A. Ratcliff, J. Luecke, X. He, B. T. Zigler, A. M. Dean, Ignition quality tester (IQT) investigation of the negative temperature coefficient region of alkane autoignition, Energy & Fuels 27 (3) (2013) 1632–1642. doi:10.1021/ef301738b.

[36] G. E. Bogin Jr., E. Osecky, J. Chen, M. A. Ratcliff, J. Luecke, B. T. Zigler, A. M. Dean, Experiments and computational fluid dynamics modeling analysis of large n-alkane ignition kinetics in the ignition quality tester, Energy & Fuels 28 (7) (2014) 4781–4794. doi:10.1021/ef500769j.

[37] E. M. Osecky, G. E. Bogin Jr., S. M. Villano, M. A. Ratcliff, J. Luecke, B. T. Zigler, A. M. Dean, Investigation of iso-octane ignition and validation

of a multizone modeling method in an ignition quality tester, Energy & Fuels 30 (11) (2016) 9761–9771. doi:10.1021/acs.energyfuels.6b01406.

[38] G. E. Bogin, J. Luecke, M. A. Ratcliff, E. Osecky, B. T. Zigler, Effects of iso-octane/ethanol blend ratios on the observance of negative temperature coefficient behavior within the ignition quality tester, Fuel 186 (2016) 82–90. doi:10.1016/j.fuel.2016.08.021.

[39] A. Tekawade, M. A. Oehlschlaeger, An experimental study of the spray ignition of alkanes, Fuel 185 (2016) 381–393. doi:10.1016/j.fuel.2016.07.108.

[40] B. T. Fisher, J. C. Allen, R. L. Hancock, J. A. Bittle, Evaluating the potential of a direct-injection constant-volume combustion chamber as a tool to validate chemical-kinetic models for liquid fuels, Combustion Science and Technology 189 (1) (2017) 1–23. doi:10.1080/00102202.2016.1193015.

[41] R. Minetti, M. Ribaucour, M. Carlier, L. Sochet, Autoignition delays of a series of linear and branched chain alkanes in the intermediate range of temperature, Combustion science and technology 113 (1) (1996) 179–192. doi:10.1080/00102209608935493.

[42] R. D. Wilk, R. S. Cohen, N. P. Cernansky, Oxidation of *n*-butane: transition in the mechanism across the region of negative temperature coefficient, Industrial & engineering chemistry research 34 (7) (1995) 2285–2297. doi:10.1021/ie00046a010.

[43] W. Liang, C. K. Law, Theory of first-stage ignition delay in hydrocarbon NTC chemistry, Combustion and Flame 188 (2018) 162–169. doi:10.1016/j.combustflame.2017.10.003.

[44] S. Y. Yang, N. Naser, S. H. Chung, J. Cha, Effect of temperature, pressure and equivalence ratio on ignition delay in ignition quality tester (IQT): Diesel, n-heptane, and iso-octane fuels under low temperature conditions, SAE International Journal of Fuels and Lubricants 8 (2015) 537–548. doi:10.4271/2015-01-9074.

[45] G. E. Bogin Jr, A. DeFilippo, J.-Y. Chen, G. Chin, J. Luecke, M. A. Ratcliff, B. T. Zigler, A. M. Dean, Numerical and experimental investigation of n-heptane autoignition in the ignition quality tester (IQT), Energy & Fuels 25 (12) (2011) 5562–5572. doi:10.1021/ef201079g.

[46] M. J. Mubarak Ali, A. Elhagrasy, M. Sarathy, S. Chung, H. G. Im, Auto-ignition and spray characteristics of *n*-heptane and *iso*-octane fuels in ignition quality tester, SAE Technical Paper 2018-01-0299 (2018). doi:10.4271/2018-01-0299.

[47] J. L. Mendelson, Ignition quality tester characterization with pure component and conventional navy fuels, Ph.D. thesis, University of Maryland, College Park (2016). doi:10.13016/M2QK01.

[48] J. Herzler, M. Fikri, K. Hitzbleck, R. Starke, C. Schulz, P. Roth, G. Kalghatgi, Shock-tube study of the autoignition of n-heptane/toluene/air mixtures at intermediate temperatures and high pressures, Combustion and flame 149 (1) (2007) 25–31. doi:10.1016/j.combustflame.2006.12.015.

[49] G. Kalghatgi, R. Head, J. Chang, Y. Viollet, H. Babiker, A. Amer, An alternative method based on toluene/n-heptane surrogate fuels for rating the anti-knock quality of practical gasolines, SAE International Journal of Fuels and Lubricants 2014-01-2609. doi:10.4271/2014-01-2609.

[50] N. Morgan, A. Smallbone, A. Bhave, M. Kraft, R. Cracknell, G. Kalghatgi, Mapping surrogate gasoline compositions into RON/MON space, Combustion and Flame 157 (6) (2010) 1122–1131. doi:10.1016/j.combustflame.2010.02.003.

[51] G. Kalghatgi, H. Babiker, J. Badra, A simple method to predict knock using toluene, iso-octane, n-heptane blends (TPRF) as gasoline surrogates, SAE International Journal of Engines 7 (2015) 663–672. doi:10.4271/2015-01-0757.

[52] V. Kalaskar, D. Kang, A. L. Boehman, Impact of fuel composition and intake pressure on lean autoignition of surrogate gasoline fuels in a CFR engine, Energy & Fuels 31 (10) (2017) 11315–11327. doi:10.1021/acs.energyfuels.7b01157.

[53] E. Singh, J. Badra, M. Mehl, S. M. Sarathy, Chemical kinetic insights into the octane number and octane sensitivity of gasoline surrogate mixtures, Energy & Fuels 31 (2) (2017) 1945–1960. doi:10.1021/acs.energyfuels.6b02659.

[54] S. M. Sarathy, G. Kukkadapu, M. Mehl, T. Javed, A. Ahmed, N. Naser, A. Tekawade, G. Kosiba, M. AlAbbad, E. Singh, et al., Compositional effects on the ignition of FACE gasolines, Combustion and Flame 169 (2016) 171–193. doi:10.1016/j.combustflame.2016.04.010.

[55] W. Cannella, M. Foster, G. Gunter, W. Leppard, FACE gasolines and blends with ethanol: detailed characterization of physical and chemical properties (2014).
URL http://www.crcao.com/reports/recentstudies2014/AVFL-24/AVFL-24%20FACE%20Gasolines%20Report%20-%20071414.pdf

[56] L. N. Allard, G. D. Webster, T. W. Ryan, A. C. Matheaus, G. Baker, A. Beregszaszy, H. Read, K. Mortimer, G. Jones, Diesel fuel ignition quality as determined in the ignition quality tester (IQT^{TM})- Part IV, SAE technical paper 2001-01-3527 (2001). doi:10.4271/2001-01-3527.

[57] G. Knothe, A. C. Matheaus, T. W. Ryan, Cetane numbers of branched and straight-chain fatty esters determined in an ignition quality tester, Fuel 82 (8) (2003) 971–975. doi:10.1016/S0016-2361(02)00382-4.

[58] M. Lapuerta, M. Villajos, J. R. Agudelo, A. L. Boehman, Key properties and blending strategies of hydrotreated vegetable oil as biofuel for diesel engines, Fuel processing technology 92 (12) (2011) 2406–2411. doi:10.1016/j.fuproc.2011.09.003.

[59] Z. Zheng, T. Badawy, N. Henein, E. Sattler, Investigation of physical and chemical delay periods of different fuels in the ignition quality tester, Journal of Engineering for Gas Turbines and Power 135 (061501). doi:10.1115/1.4023607.

[60] M. Dahmen, W. Marquardt, A novel group contribution method for the prediction of the derived cetane number of oxygenated hydrocarbons, Energy & Fuels 29 (9) (2015) 5781–5801. doi:10.1021/acs.energyfuels.5b01032.

[61] J. E. Dec, Advanced compression-ignition enginesunderstanding the in-cylinder processes, Proceedings of the combustion institute 32 (2) (2009) 2727–2742. doi:10.1016/j.proci.2008.08.008.

[62] S. Saxena, I. D. Bedoya, Fundamental phenomena affecting low temperature combustion and HCCI engines, high load limits and strategies for extending

these limits, Progress in Energy and Combustion Science 39 (5) (2013) 457–488. doi:10.1016/j.pecs.2013.05.002.

[63] A. B. Dempsey, S. J. Curran, R. M. Wagner, A perspective on the range of gasoline compression ignition combustion strategies for high engine efficiency and low nox and soot emissions: Effects of in-cylinder fuel stratification, International Journal of Engine Research 17 (8) (2016) 897–917. doi:10.1177/1468087415621805.

[64] A. K. Agarwal, Biofuels (alcohols and biodiesel) applications as fuels for internal combustion engines, Progress in energy and combustion science 33 (3) (2007) 233–271. doi:10.1016/j.pecs.2006.08.003.

[65] G. Knothe, Biodiesel and renewable diesel: a comparison, Progress in energy and combustion science 36 (3) (2010) 364–373. doi:doi.org/10.1016/j.pecs.2009.11.004.

[66] G. Knothe, L. F. Razon, Biodiesel fuels, Progress in Energy and Combustion Science 58 (2017) 36–59. doi:10.1016/j.pecs.2016.08.001.

[67] A. K. Agarwal, J. G. Gupta, A. Dhar, Potential and challenges for large-scale application of biodiesel in automotive sector, Progress in Energy and Combustion Science 61 (2017) 113–149. doi:10.1016/j.pecs.2017.03.002.

[68] C. J. Mueller, W. J. Cannella, J. T. Bays, T. J. Bruno, K. DeFabio, H. D. Dettman, R. M. Gieleciak, M. L. Huber, C.-B. Kweon, S. S. McConnell, W. J. Pitz, M. A. Ratcliff, Diesel surrogate fuels for engine testing and chemical-kinetic modeling: Compositions and properties, Energy & Fuels 30 (2) (2016) 1445–1461. doi:10.1021/acs.energyfuels.5b02879.

[69] K. V. Puduppakkam, L. Liang, C. V. Naik, E. Meeks, S. L. Kokjohn, R. D. Reitz, Use of detailed kinetics and advanced chemistry-solution techniques in CFD to investigate dual-fuel engine concepts, SAE International Journal of Engines 4 (2011-01-0895) (2011) 1127–1149. doi:10.4271/2011-01-0895.

[70] W. J. Pitz, C. J. Mueller, Recent progress in the development of diesel surrogate fuels, Progress in Energy and Combustion Science 37 (3) (2011) 330–350. doi:10.1016/j.pecs.2010.06.004.

[71] J. Badra, A. S. AlRamadan, S. M. Sarathy, Optimization of the octane response of gasoline/ethanol blends, Applied Energy 203 (2017) 778–793. doi:10.1016/j.apenergy.2017.06.084.

[72] H. Abou-Rachid, L. Bonneviot, G. Xu, S. Kaliaguine, On the correlation between kinetic rate constants in the auto-ignition process of some oxygenates and their cetane number: a quantum chemical study, Journal of Molecular Structure: THEOCHEM 621 (3) (2003) 293–304. doi:dx.doi.org/10.1016/S0166-1280(02)00676-0.

[73] K. J. Morganti, T. M. Foong, M. J. Brear, G. da Silva, Y. Yang, F. L. Dryer, The research and motor octane numbers of liquefied petroleum gas (LPG), Fuel 108 (2013) 797–811. doi:10.1016/j.fuel.2013.01.072.

[74] J. Yanowitz, M. A. Ratcliff, R. L. McCormick, J. D. Taylor, M. J. Murphy, Compendium of experimental cetane numbers, Technical Repot. National Renewable Energy Laboratory.

[75] J. Guibet, Carburants et moteurs, tome 1 et 2, publications de lInstitut Français du Pétrole, ed, Technip, Paris.

[76] V. Simanzhenkov, R. Idem, Crude oil chemistry, CRC Press, 2003.

[77] A. G. Abdul Jameel, N. Naser, A.-H. Emwas, S. Dooley, S. M. Sarathy, Predicting fuel ignition quality using 1H NMR spectroscopy and multiple linear regression, Energy & Fuels 30 (11) (2016) 9819–9835. doi:10.1021/acs.energyfuels.6b01690.

[78] R. C. Santana, P. T. Do, M. Santikunaporn, W. E. Alvarez, J. D. Taylor, E. L. Sughrue, D. E. Resasco, Evaluation of different reaction strategies for the improvement of cetane number in diesel fuels, Fuel 85 (5) (2006) 643–656. doi:10.1016/j.fuel.2005.08.028.

[79] Knocking characteristics of pure hydrocarbons, ASTM International.doi:10.1520/STP225-EB.

[80] P. Hellier, N. Ladommatos, R. Allan, S. Filip, J. Rogerson, The importance of double bond position and cis–trans isomerisation in diesel combustion and emissions, Fuel 105 (2013) 477–489. doi:10.1016/j.fuel.2012.08.007.

[81] R. Stone, Introduction to internal combustion engines, Springer, 1999. doi:10.1007/978-1-349-14916-2.

[82] A. De Klerk, Fischer-Tropsch Refining, John Wiley & Sons, 2012. doi:10.1002/9783527635603.

[83] W. L. Kubic Jr, A group contribution method for estimating cetane and octane numbers, Tech. rep., Los Alamos National Lab.(LANL), Los Alamos, NM (United States) (2016).

[84] I. Hunwartzen, Modification of CFR test engine unit to determine octane numbers of pure alcohols and gasoline-alcohol blends, SAE Technical Paper 820002 (1982). doi:10.4271/820002.

[85] E. Christensen, J. Yanowitz, M. Ratcliff, R. L. McCormick, Renewable oxygenate blending effects on gasoline properties, Energy & Fuels 25 (10) (2011) 4723–4733. doi:10.1021/es402793p.

[86] F. M. Haas, A. Ramcharan, F. L. Dryer, Relative reactivities of the isomeric butanols and ethanol in an ignition quality tester, Energy & Fuels 25 (9) (2011) 3909–3916. doi:10.1021/ef2008024.

[87] A. S. AlRamadan, J. Badra, T. Javed, M. Al-Abbad, N. Bokhumseen, P. Gaillard, H. Babiker, A. Farooq, S. M. Sarathy, Mixed butanols addition to gasoline surrogates: Shock tube ignition delay time measurements and chemical kinetic modeling, Combustion and Flame 162 (10) (2015) 3971–3979. doi:10.1016/j.combustflame.2015.07.035.

[88] S. Y. Yang, N. Naser, S. H. Chung, K. Al-Qurashi, Ignition delay and soot oxidative reactivity of MTBE blended diesel fuel, SAE technical paper 2014-01-1266 (2014). doi:10.4271/2014-01-1266.

[89] A. Brassat, M. Thewes, M. Müther, S. Pischinger, C. Lee, R. X. Fernandes, H. Olivier, Y. Uygun, Analysis of the effects of certain alcohol and furan-based biofuels on controlled auto ignition, SAE Technical Paper 2012-01-1135 (2012). doi:10.4271/2012-01-1135.

[90] A. Sudholt, L. Cai, J. Heyne, F. M. Haas, H. Pitsch, F. L. Dryer, Ignition characteristics of a bio-derived class of saturated and unsaturated furans for

engine applications, Proceedings of the Combustion Institute 35 (3) (2015) 2957–2965. doi:10.1016/j.proci.2014.06.147.

[91] Y. Román-Leshkov, C. J. Barrett, Z. Y. Liu, J. A. Dumesic, Production of dimethylfuran for liquid fuels from biomass-derived carbohydrates, Nature 447 (7147) (2007) 982–985. doi:10.1038/nature05923.

[92] G. K. Lilik, A. L. Boehman, Effects of fuel ignition quality on critical equivalence ratio for autoignition, Energy & Fuels 27 (3) (2013) 1586–1600. doi:10.1021/ef301600h.

[93] G. K. Lilik, A. L. Boehman, Effects of fuel composition on critical equivalence ratio for autoignition, Energy & Fuels 27 (3) (2013) 1601–1612. doi:10.1021/ef3016014.

[94] A. Ramcharan, Formulation of a biodiesel surrogate fuel through investigation of the ignition delay using an ignition quality tester (2011).

[95] S. M. Sarathy, C. K. Westbrook, M. Mehl, W. J. Pitz, C. Togbe, P. Dagaut, H. Wang, M. A. Oehlschlaeger, U. Niemann, K. Seshadri, et al., Comprehensive chemical kinetic modeling of the oxidation of 2-methylalkanes from c 7 to c 20, Combustion and flame 158 (12) (2011) 2338–2357. doi:10.1016/j.combustflame.2011.05.007.

[96] J. S. Heyne, A. L. Boehman, S. Kirby, Autoignition studies of trans-and cis-decalin in an ignition quality tester (IQT) and the development of a high thermal stability unifuel/single battlefield fuel, Energy & Fuels 23 (12) (2009) 5879–5885. doi:10.1021/ef900715m.

[97] T. G. Smagala, E. Christensen, K. M. Christison, R. E. Mohler, E. Gjersing, R. L. McCormick, Hydrocarbon renewable and synthetic diesel fuel blendstocks: composition and properties, Energy & Fuels 27 (1) (2012) 237–246. doi:10.1021/ef3012849.

[98] S. H. Won, S. Dooley, P. S. Veloo, H. Wang, M. A. Oehlschlaeger, F. L. Dryer, Y. Ju, The combustion properties of 2, 6, 10-trimethyl dodecane and a chemical functional group analysis, Combustion and Flame 161 (3) (2014) 826–834. doi:10.1016/j.combustflame.2013.08.010.

[99] G. Knothe, "Designer" biodiesel: optimizing fatty ester composition to improve fuel properties, Energy & Fuels 22 (2) (2008) 1358–1364. doi:10.1021/ef700639e.

[100] G. Knothe, Fuel properties of methyl esters of borage and black currant oils containing methyl γ-linolenate, European Journal of Lipid Science and Technology 115 (8) (2013) 901–908. doi:10.1002/ejlt.201300061.

[101] G. Knothe, A comprehensive evaluation of the cetane numbers of fatty acid methyl esters, Fuel 119 (2014) 6–13. doi:10.1016/j.fuel.2013.11.020.

[102] G. Knothe, Fuel properties of highly polyunsaturated fatty acid methyl esters. prediction of fuel properties of algal biodiesel, Energy & Fuels 26 (8) (2012) 5265–5273. doi:10.1021/ef300700v.

[103] B. R. Moser, G. Knothe, S. C. Cermak, Biodiesel from meadowfoam (*Limnanthes alba* L.) seed oil: oxidative stability and unusual fatty acid composition, Energy & Environmental Science 3 (3) (2010) 318–327. doi:10.1039/B923740M.

Supplementary Material

Table S1: Fuel matrix of PRF, TRF and TPRF

Fuel	PRF	Volume fraction			RON	MON	Ref.
		Toluene	*iso*-Octane	*n*-Heptane			
PRF 0	0	0.000	0.000	1.000	0.0	0.0	[6, 7]
PRF 10	10	0.000	0.100	0.900	10.0	10.0	[6, 7]
PRF 20	20	0.000	0.200	0.800	20.0	20.0	[6, 7]
PRF 30	30	0.000	0.300	0.700	30.0	30.0	[6, 7]
PRF 40	40	0.000	0.400	0.600	40.0	40.0	[6, 7]
PRF 50	50	0.000	0.500	0.500	50.0	50.0	[6, 7]
PRF 60	60	0.000	0.600	0.400	60.0	60.0	[6, 7]
PRF 70	70	0.000	0.700	0.300	70.0	70.0	[6, 7]
PRF 80	80	0.000	0.800	0.200	80.0	80.0	[6, 7]
PRF 83	83	0.000	0.830	0.170	83.0	83.0	[6, 7]
PRF 90	90	0.000	0.900	0.100	90.0	90.0	[6, 7]
PRF 95	95	0.000	0.950	0.050	95.0	95.0	[6, 7]
PRF 100	100	0.000	1.000	0.000	100.0	100.0	[6, 7]
TRF 40	0	0.400	0.000	0.600	53.7	47.1	BR[a]
TRF 45	0	0.450	0.000	0.550	59.7	52.4	BR
TRF 50	0	0.500	0.000	0.500	65.1	58.0	[49]
TRF 55	0	0.550	0.000	0.450	71.3	62.6	BR
TRF 60	0	0.600	0.000	0.400	77.9	68.5	[49]
TRF 65	0	0.650	0.000	0.350	84.5	74.5	[49]
TRF 70	0	0.700	0.000	0.300	89.3	78.2	[49]
TPRF 10-54	60	0.100	0.540	0.360	66.0	64.4	[51]
TPRF 20-48	60	0.200	0.480	0.320	73.6	70.0	[51]
TPRF 30-42	60	0.300	0.420	0.280	79.0	74.0	[51]
TPRF 40-36	60	0.400	0.360	0.240	86.2	79.6	[51]
TPRF 10-63	70	0.100	0.630	0.270	74.8	72.8	BR
TPRF 20-56	70	0.200	0.560	0.240	80.7	76.9	BR
TPRF 30-49	70	0.300	0.490	0.210	86.1	80.6	BR
TPRF 40-42	70	0.400	0.420	0.180	91.0	84.0	BR
TPRF 10-72	80	0.100	0.720	0.180	84.5	82.0	[51]
TPRF 20-64	80	0.200	0.640	0.160	89.1	85.6	[51]
TPRF 30-56	80	0.300	0.560	0.140	92.8	86.9	[51]
TPRF 40-48	80	0.400	0.480	0.120	96.7	88.7	[51]
TPRF 10-81	90	0.100	0.810	0.090	92.0	90.0	BR
TPRF 10-72	90	0.200	0.720	0.080	95.3	91.4	BR
TPRF 10-63	90	0.300	0.630	0.070	98.3	92.7	BR

[a] BR indicates blending rule in [51]

Table S2: Fuel matrix of multi component surrogate blends from [53]

Blend	Volume fraction						RON[a]	MON[a]
	Toluene	*iso*-Octane	*n*-heptane	1-Hexene	124-TMB[b]	CPT[c]		
MCSB 1	0.000	0.910	0.090	0.000	0.000	0.000	90.9	91.1
MCSB 2	0.150	0.725	0.125	0.000	0.000	0.000	90.5	88.0
MCSB 3	0.300	0.525	0.175	0.000	0.000	0.000	89.5	84.7
MCSB 4	0.000	0.847	0.051	0.102	0.000	0.000	92.9	90.2
MCSB 5	0.000	0.770	0.030	0.200	0.000	0.000	93.0	88.5
MCSB 6	0.150	0.650	0.100	0.100	0.000	0.000	91.2	86.8
MCSB 7	0.150	0.580	0.070	0.200	0.000	0.000	91.7	85.2
MCSB 8	0.319	0.465	0.139	0.077	0.000	0.000	91.4	84.9
MCSB 9	0.300	0.390	0.110	0.200	0.000	0.000	90.9	82.7
MCSB 10	0.000	0.760	0.090	0.000	0.150	0.000	94.2	90.5
MCSB 11	0.000	0.610	0.090	0.000	0.300	0.000	96.8	90.0
MCSB 12	0.080	0.750	0.100	0.000	0.070	0.000	93.3	90.1
MCSB 13	0.150	0.575	0.125	0.000	0.150	0.000	94.4	88.4
MCSB 14	0.000	0.810	0.090	0.000	0.000	0.100	94.1	91.4
MCSB 15	0.000	0.710	0.090	0.000	0.000	0.200	97.5	90.7
MCSB 16	0.150	0.620	0.130	0.000	0.000	0.100	93.0	88.0
MCSB 17	0.300	0.430	0.170	0.000	0.000	0.100	91.7	85.5
MCSB 18	0.150	0.510	0.140	0.000	0.000	0.200	94.5	87.8
MCSB 19	0.300	0.320	0.180	0.000	0.000	0.200	92.9	85.3
MCSB 20	0.000	0.700	0.300	0.000	0.000	0.000	70.2	70.0
MCSB 21	0.150	0.520	0.330	0.000	0.000	0.000	71.2	69.0
MCSB 22	0.300	0.300	0.400	0.000	0.000	0.000	68.4	63.7
MCSB 23	0.000	0.650	0.250	0.100	0.000	0.000	74.2	72.6
MCSB 24	0.000	0.570	0.230	0.200	0.000	0.000	74.6	72.0
MCSB 25	0.150	0.440	0.310	0.100	0.000	0.000	72.0	68.0
MCSB 26	0.150	0.360	0.290	0.200	0.000	0.000	72.0	67.2
MCSB 27	0.000	0.570	0.280	0.000	0.150	0.000	77.8	74.6
MCSB 28	0.000	0.410	0.290	0.000	0.300	0.000	83.0	77.7
MCSB 29	0.080	0.540	0.310	0.000	0.070	0.000	73.5	71.8
MCSB 30	0.177	0.360	0.340	0.000	0.124	0.000	76.7	72.0

[a] ASTM D2699, D2700 measurements [6, 7] performed at Saudi Aramco [53]

[b] 1,2,4-trimethylbenzene

[c] Cyclopentane

Table S3: Fuel matrix of FACE and certification gasoline fuels

Fuel	RON	MON	Ref.
FACE A gasoline	83.5	83.6	COA[a]
FACE C gasoline	84.7	83.6	COA
FACE F gasoline	94.4	88.8	COA
FACE G gasoline	96.8	85.8	COA
FACE I gasoline	70.3	69.6	COA
FACE J gasoline	71.8	68.8	COA
Coryton gasoline	97.5	86.6	COA
Haltermann gasoline	91.0	83.4	COA

[a] Certificate of analysis

Table S4: Fuel matrix of FACE blended with ethanol

Fuel	Volume fraction		RON[1]	MON[1]
	Fuel	Ethanol		
FACE A	0.90	0.10	92.0	88.0
	0.75	0.25	100.7	90.6
	0.60	0.40	104.1	91.7
	0.40	0.60	106.0	91.3
FACE C	0.90	0.10	92.2	87.1
	0.75	0.25	100.3	90.5
	0.60	0.40	104.1	91.0
	0.40	0.60	105.8	91.3
FACE F	0.90	0.10	98.9	88.5
	0.75	0.25	103.2	89.5
	0.60	0.40	104.7	90.3
	0.40	0.60	105.7	90.5
FACE G	0.90	0.10	98.8	86.1
	0.75	0.25	102.4	87.9
	0.60	0.40	100.4	88.3
	0.40	0.60	104.1	89.7
FACE I	0.90	0.10	79.9	78.0
	0.75	0.25	92.6	85.3
	0.60	0.40	100.4	88.3
	0.40	0.60	104.1	89.7
FACE J	0.90	0.10	79.0	73.6
	0.75	0.25	89.8	81.7
	0.60	0.40	98.0	85.9
	0.40	0.60	103.6	88.2

[1] ASTM D2699, D2700 measurements [6, 7] performed at Saudi Aramco [71]

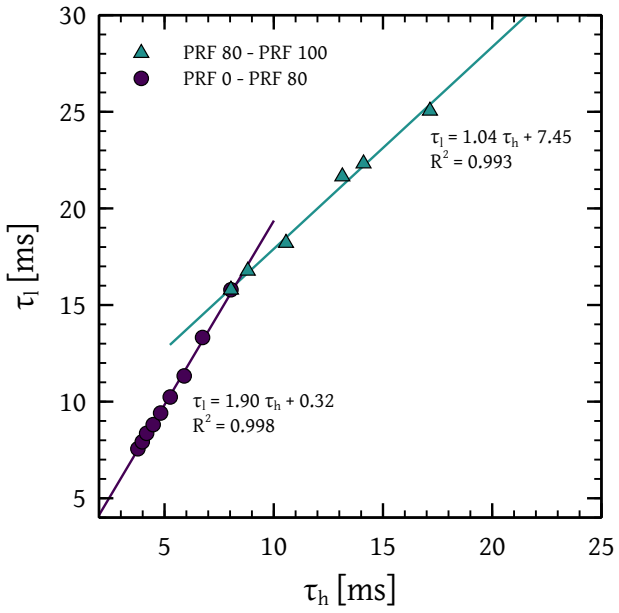

Figure S1: Variation of IDTs of PRFs at DCN and τ_l temperatures

Table S5: Ignition delay time sensitivity and RON/MON/OS predictions of all fuels

	Fuel/Mixture	τ_h [ms]	τ_l [ms]	DCN	$\tau_{l,PRF}$ [ms]	IDS	Predicted			Nominal			RON/MON Ref.
							RON	MON	OS	RON	MON	OS	
PRF	PRF 0	3.78	7.56	53.8	7.51	1.0063	1.2	1.0	0.3	0.0	0.0	0.0	[6, 7]
	PRF 10	3.98	7.90	51.3	7.95	0.9940	10.2	10.4	-0.2	10.0	10.0	0.0	[6, 7]
	PRF 20	4.18	8.34	49.1	8.37	0.9969	17.9	18.1	-0.1	20.0	20.0	0.0	[6, 7]
	PRF 30	4.48	8.90	46.1	8.97	0.9925	27.8	28.1	-0.3	30.0	30.0	0.0	[6, 7]
	PRF 40	4.82	9.71	43.2	9.62	1.0097	37.0	36.7	0.4	40.0	40.0	0.0	[6, 7]
	PRF 50	5.23	10.49	40.1	10.37	1.0120	46.0	45.5	0.5	50.0	50.0	0.0	[6, 7]
	PRF 60	5.90	11.64	36.1	11.53	1.0099	57.2	56.8	0.4	60.0	60.0	0.0	[6, 7]
	PRF 70	6.82	12.88	31.6	13.03	0.9886	68.5	69.0	-0.5	70.0	70.0	0.0	[6, 7]
	PRF 80	8.17	15.02	27.7	15.11	0.9939	77.3	77.5	-0.2	80.0	80.0	0.0	[6, 7]
	PRF 83	8.81	16.07	26.3	16.07	1.0003	80.2	80.2	0.0	81.0	81.0	0.0	[6, 7]
	PRF 90	10.56	18.73	23.3	18.60	1.0069	86.1	85.9	0.3	90.0	90.0	0.0	[6, 7]
	PRF 95	13.84	22.87	19.6	23.19	0.9862	92.6	93.2	-0.6	95.0	95.0	0.0	[6, 7]
	PRF 100	17.06	27.66	17.4	27.59	1.0027	96.3	96.1	0.1	100.0	100.0	0.0	[6, 7]
TRF	TRF 40	5.78	12.95	36.7	11.32	1.1437	55.4	50.7	4.7	53.7	47.1	6.6	BR[a]
	TRF 45	6.37	14.22	33.8	12.30	1.1557	63.2	58.2	5.0	59.7	52.4	7.3	BR[a]
	TRF 50	6.99	16.40	31.0	13.30	1.2334	69.9	63.1	6.8	65.1	58.0	7.1	[49]
	TRF 55	7.79	18.35	28.6	14.54	1.2624	75.2	67.8	7.4	71.3	62.6	8.7	BR[a]
	TRF 60	9.04	20.80	25.8	16.40	1.2680	81.2	73.7	7.5	77.9	68.5	9.4	[49]
	TRF 65	10.80	23.57	22.9	18.94	1.2442	86.8	79.8	7.0	84.5	74.5	10.0	[49]
	TRF 70	13.60	32.07	19.8	22.86	1.4029	92.2	82.5	9.8	89.3	78.2	11.1	[49]
TPRF	TPRF 60-10	6.63	14.32	32.2	12.72	1.1254	66.9	62.7	4.2	66.0	64.4	1.6	[51]
	TPRF 60-20	7.62	16.14	29.1	14.28	1.1306	74.2	69.9	4.3	73.6	70.0	3.6	[51]
	TPRF 60-30	8.84	18.71	26.2	16.11	1.1614	80.4	75.2	5.1	79.0	74.0	5.0	[51]
	TPRF 60-40	10.98	22.45	22.7	19.20	1.1693	87.2	81.9	5.3	86.2	79.6	6.6	[51]
	TPRF 70-10	7.68	15.68	28.9	14.37	1.0913	74.6	71.4	3.2	74.8	72.8	2.0	BR[a]
	TPRF 70-20	8.81	17.37	26.3	16.07	1.0812	80.2	77.4	2.9	80.7	76.9	3.8	BR[a]
	TPRF 70-30	10.27	20.90	23.7	18.19	1.1491	85.3	80.5	4.8	86.1	80.6	5.5	BR[a]
	TPRF 70-40	13.49	28.49	19.9	22.71	1.2546	92.1	84.9	7.2	91.0	84.0	7.0	BR[a]
	TPRF 80-10	9.27	18.12	25.4	16.74	1.0824	82.1	79.1	2.9	84.5	82.0	2.5	[51]
	TPRF 80-20	10.86	20.44	22.8	19.03	1.0741	86.9	84.3	2.7	89.1	85.6	3.5	[51]
	TPRF 80-30	13.70	27.52	19.8	23.00	1.1966	92.4	86.4	6.0	92.8	86.9	5.9	[51]
	TPRF 80-40	18.66	37.31	16.5	29.75	1.2542	97.6	90.3	7.2	96.7	88.7	8.0	[51]

Continued on next page

Table S5: (continued) Predicted RON from DCN obtained from literature and experiments in present work compared to nominal RON

	Fuel/Mixture	τ_h [ms]	τ_l [ms]	DCN	$\tau_{l,PRF}$ [ms]	IDS	Predicted			Nominal			RON/MON Ref.
							RON	MON	OS	RON	MON	OS	
TPRF	TPRF 90-10	12.35	20.56	21.1	21.13	0.9732	90.2	91.3	-1.1	92.0	90.0	2.0	BR[a]
	TPRF 90-20	15.56	27.86	18.3	25.55	1.0905	94.8	91.6	3.2	95.3	91.4	3.9	BR[a]
	TPRF 90-30	20.65	38.78	15.6	32.42	1.1961	98.9	92.9	6.0	98.3	92.7	5.6	BR[a]
MCSB	MCSB 1	10.60	19.14	23.2	18.66	1.0257	86.3	85.3	1.0	90.9	91.1	-0.2	[53]
	MCSB 2	11.71	24.71	21.8	20.23	1.2215	88.9	82.4	6.5	90.5	88.0	2.5	[53]
	MCSB 3	11.88	27.00	21.6	20.47	1.3191	89.2	80.8	8.4	89.5	84.7	4.8	[53]
	MCSB 4	12.11	22.87	21.3	20.79	1.1000	89.7	86.2	3.5	92.9	90.2	2.7	[53]
	MCSB 5	12.36	23.70	21.0	21.14	1.1211	90.2	86.1	4.1	93.0	88.5	4.5	[53]
	MCSB 6	11.89	22.56	21.6	20.48	1.1014	89.3	85.8	3.5	91.2	86.8	4.4	[53]
	MCSB 7	12.33	25.38	21.1	21.10	1.2030	90.1	84.0	6.1	91.7	85.2	6.5	[53]
	MCSB 8	12.50	24.95	20.9	21.34	1.1694	90.4	85.1	5.3	91.4	84.9	6.5	[53]
	MCSB 9	12.40	28.43	21.0	21.20	1.3413	90.3	81.4	8.8	90.9	82.7	8.2	[53]
	MCSB 10	12.46	26.17	20.9	21.28	1.2298	90.4	83.6	6.7	94.2	90.5	3.7	[53]
	MCSB 11	14.40	28.40	19.2	23.96	1.1852	93.4	87.6	5.7	96.8	90.0	6.8	[53]
	MCSB 12	12.09	26.40	21.3	20.76	1.2717	89.7	82.1	7.6	93.3	90.1	3.2	[53]
	MCSB 13	13.10	24.64	20.3	22.17	1.1115	91.5	87.7	3.8	94.4	88.4	6.0	[53]
	MCSB 14	14.09	24.93	19.4	23.54	1.0593	93.0	90.8	2.2	94.1	91.4	2.7	[53]
	MCSB 15	17.74	34.32	17.0	28.51	1.2039	96.8	90.7	6.2	97.5	90.7	6.8	[53]
	MCSB 16	14.02	27.84	19.5	23.44	1.1878	92.9	87.1	5.8	93.0	88.0	5.0	[53]
	MCSB 17	13.33	28.63	20.1	22.49	1.2732	91.8	84.2	7.6	91.7	85.5	6.2	[53]
	MCSB 18	16.34	39.78	17.8	26.61	1.4949	95.6	84.6	11.0	94.5	87.8	6.7	[53]
	MCSB 19	16.01	40.77	18.0	26.16	1.5584	95.2	83.5	11.8	92.9	85.3	7.6	[53]
	MCSB 20	6.80	12.98	31.6	13.00	0.9988	68.4	68.4	-0.1	70.2	70.0	0.2	[53]
	MCSB 21	6.50	13.24	33.2	12.52	1.0579	64.6	62.5	2.1	71.2	69.0	2.2	[53]
	MCSB 22	6.59	13.57	32.4	12.66	1.0719	66.5	63.9	2.6	68.4	63.7	4.7	[53]
	MCSB 23	7.01	13.74	30.9	13.33	1.0309	70.0	68.8	1.2	74.2	72.6	1.6	[53]
	MCSB 24	7.62	15.71	29.1	14.28	1.1004	74.2	70.7	3.5	74.6	72.0	2.6	[53]
	MCSB 25	7.03	14.43	30.8	13.36	1.0801	70.2	67.3	2.9	72.0	68.0	4.0	[53]
	MCSB 26	7.33	15.43	29.9	13.83	1.1158	72.3	68.4	3.9	72.0	67.2	4.8	[53]
	MCSB 29	7.10	14.20	30.6	13.47	1.0542	70.7	68.7	2.0	77.8	74.6	3.2	[53]
	MCSB 30	8.51	18.42	26.9	15.62	1.1792	78.9	73.3	5.6	83.0	77.7	5.3	[53]
	MCSB 31	6.75	13.21	31.8	12.92	1.0227	67.9	67.1	0.9	73.5	71.8	1.7	[53]
	MCSB 32	7.38	15.16	29.8	13.91	1.0902	72.7	69.5	3.2	76.7	72.0	4.7	[53]

Continued on next page

Table S5: (continued) Predicted RON from DCN obtained from literature and experiments in present work compared to nominal RON

	Fuel/Mixture	τ_h [ms]	τ_l [ms]	DCN	$\tau_{l,PRF}$ [ms]	IDS	Predicted			Nominal			RON/MON Ref.
							RON	MON	OS	RON	MON	OS	
Practical gasolines	FACE A gasoline	8.75	16.59	26.4	15.98	1.0384	80.0	78.5	1.5	83.5	83.6	-0.1	COA[b]
	FACE C gasoline	8.69	16.87	26.5	15.89	1.0618	79.7	77.5	2.3	84.7	83.6	1.1	COA[b]
	FACE F gasoline	14.45	30.33	19.1	24.03	1.2622	93.4	86.1	7.4	94.4	88.8	5.6	COA[b]
	FACE G gasoline	15.99	35.60	18.0	26.13	1.3622	95.2	86.1	9.1	96.8	85.8	11.0	COA[b]
	FACE I gasoline	6.78	14.01	31.7	12.96	1.0807	68.2	65.3	2.9	70.3	69.6	0.7	COA[b]
	FACE J gasoline	7.39	16.17	29.7	13.92	1.1615	72.7	67.6	5.1	71.8	68.8	3.0	COA[b]
	Coryton gasoline	17.22	41.48	17.3	27.80	1.4919	96.4	85.4	11.0	97.5	86.6	10.9	COA[b]
	Haltermann gasoline	13.13	32.24	20.3	22.21	1.4516	91.5	81.1	10.4	91.0	83.4	7.6	COA[b]
FACE gasolines + ethanol	FACE A + ethanol (10 vol%)	13.22	27.69	20.2	22.33	1.2398	91.7	84.7	6.9	92.0	88.0	4.0	[71]
	FACE A + ethanol (25 vol%)	23.11	47.16	14.7	35.71	1.3207	100.2	91.7	8.5	100.7	90.6	10.1	[71]
	FACE A + ethanol (40 vol%)	54.64	100.18	9.7	77.35	1.2952	106.3	98.3	8.0	104.1	91.7	12.4	[71]
	FACE C + ethanol (10 vol%)	13.98	28.75	19.5	23.38	1.2295	92.8	86.1	6.7	92.2	87.1	5.1	[71]
	FACE C + ethanol (25 vol%)	24.61	51.57	14.2	37.71	1.3676	100.8	91.6	9.2	100.3	90.5	9.8	[71]
	FACE C + ethanol (40 vol%)	57.81	113.93	9.5	81.50	1.3979	106.5	96.9	9.7	104.1	91.0	13.1	[71]
	FACE F + ethanol (10 vol%)	20.36	41.48	15.7	32.03	1.2949	98.7	90.7	8.0	98.9	88.5	10.4	[71]
	FACE F + ethanol (25 vol%)	44.59	86.22	10.6	64.12	1.3446	105.3	96.4	8.9	103.2	89.5	13.7	[71]
	FACE F + ethanol (40 vol%)	80.83	180.26	8.3	111.73	1.6134	107.8	95.5	12.3	104.7	90.3	14.4	[71]
	FACE G + ethanol (10 vol%)	23.43	49.94	14.6	36.14	1.3818	100.3	90.9	9.5	98.8	86.1	12.7	[71]
	FACE G + ethanol (25 vol%)	42.82	89.22	10.8	61.79	1.4440	105.1	94.7	10.3	102.4	87.9	14.5	[71]
	FACE G + ethanol (40 vol%)	74.59	184.03	8.5	103.54	1.7773	107.5	93.7	13.8	103.0	88.5	14.5	[71]
	FACE I + ethanol (10 vol%)	9.58	20.88	24.8	17.19	1.2143	83.2	76.8	6.4	79.9	78.0	1.9	[71]
	FACE I + ethanol (25 vol%)	15.49	36.54	18.4	25.45	1.4357	94.7	84.4	10.2	92.6	85.3	7.3	[71]
	FACE I + ethanol (40 vol%)	29.54	67.78	12.9	44.26	1.5315	102.5	91.1	11.4	100.4	88.3	12.1	[71]
	FACE I + ethanol (60 vol%)	80.62	225.64	8.3	111.45	2.0245	107.8	92.3	15.5	104.1	89.7	14.4	[71]
	FACE J + ethanol (10 vol%)	10.06	24.17	24.0	17.89	1.3513	84.7	75.7	9.0	79.0	73.6	5.4	[71]
	FACE J + ethanol (25 vol%)	15.03	37.03	18.7	24.82	1.4917	94.2	83.2	11.0	89.8	81.7	8.1	[71]
	FACE J + ethanol (40 vol%)	27.19	64.82	13.5	41.14	1.5756	101.8	89.8	11.9	98.0	85.9	12.1	[71]
	FACE J + ethanol (60 vol%)	77.81	191.12	8.4	107.76	1.7736	107.7	93.9	13.8	103.6	88.2	15.4	[71]

[a] BR indicates blending rule in [51]

[b] Certificate of analysis

Table S6: Predicted RON from DCN obtained from literature and experiments in present work compared to nominal RON

	Fuel/Mixture	Formula	DCN	DCN reference	$RON_{predicted}$	RON	RON reference
n-paraffins	Propane	C_3H_8	-20.0[1]	[72]	112.8	109.4	[73]
	n-butane	C_4H_{10}	20.6	Measurement	90.9	93.5	[73]
	n-hexane	C_6H_{14}	47.9	[74]	22.0	24.8	[75]
	n-heptane	C_7H_{16}	53.8	[24]	1.3	0.0	[6]
	n-octane	C_8H_{18}	58.2	[74]	< 0.0	< 0.0	[75]
	n-nonane	C_9H_{20}	60.9	[74]	< 0.0	< 0.0	[75]
	n-decane	$C_{10}H_{22}$	65.5	[74]	< 0.0	< 0.0	[76]
	n-dodecane	$C_{12}H_{26}$	72.9	[74]	< 0.0	< 0.0	[76]
	n-tetradecane	$C_{14}H_{30}$	85.1	[74]	< 0.0	< 0.0	[76]
iso-paraffins	2-methylbutane	C_5H_{12}	25.8	[77]	81.2	92.3	[75]
	2-methylpentane	C_6H_{14}	34.5	[74]	61.3	73.4	[75]
	2,2-dimethylbutane	C_6H_{14}	24.4	[74]	84.0	91.8	[75]
	3-methylpentane	C_6H_{14}	30.7	[77]	70.5	74.5	[75]
	2-methylhexane	C_7H_{16}	43.5	[74]	36.0	42.4	[75]
	3-methylhexane	C_7H_{16}	42.2	[77]	39.9	42.4	[75]
	2,2,3-trimethylbutane	C_7H_{16}	12.9	[74]	102.5	112.1	[75]
	2,3-dimethylpentane	C_7H_{16}	21.7	[77]	89.0	91.1	[75]
	2,4-dimethylpentane	C_7H_{16}	28.2	[77]	76.2	83.1	[75]
	3-ethylpentane	C_7H_{16}	34.1	[74]	62.3	65.0	[75]
	2-methylheptane	C_8H_{18}	47.0	[78]	24.9	21.7	[75]
	2,2,4-trimethylpentane	C_8H_{18}	17.4	[24]	96.2	100.0	[6]
Olefins	2-methyl-1,3-butadiene	C_5H_8	13.0	[60]	102.4	99.1	[79]
	1-hexene	C_6H_{12}	25.8	[74]	81.2	76.4	[75]
	1-heptene	C_7H_{14}	32.0	[74]	67.5	54.5	[75]
	2,5-dimethyl-2,4-hexadiene	C_8H_{14}	19.9	[60]	92.1	94.3	[79]
	1-octene	C_8H_{16}	40.0	[74]	46.4	28.7	[75]
	3-octene[2]	C_8H_{16}	34.0	[80]	62.5	72.5[2]	[75]

Continued on next page

Table S6: (continued) Predicted RON from DCN obtained from literature and experiments in present work compared to nominal RON

	Fuel/Mixture	Formula	DCN	DCN reference	$RON_{predicted}$	RON	RON reference
Cycloalkanes	Cyclopentane	C_5H_{10}	6.1	[74]	109.8	101.0	[81]
	Cyclohexane	C_6H_{12}	20.0	[60]	92.0	83.0	[75]
	Methylcyclopentane	C_6H_{12}	17.2	[74]	96.5	91.3	[75]
	Methylcyclohexane	C_7H_{14}	23.5	[2]	85.7	74.8	[82]
	Cyclooctane	C_8H_{16}	22.3	[74]	87.9	71.0	[81]
	Ethylcyclohexane	C_8H_{16}	35.8	[74]	57.9	46.5	[83]
	1,2,4-trimethylcyclohexane	C_9H_{18}	24.4	[60]	84.0	72.9	[83]
	1,3,5-trimethylcyclohexane	C_9H_{18}	30.5	[74, 78]	71.0	63.8	[83]
Cycloalkenes	Cyclohexene	C_6H_{10}	18.1	[60]	95.1	83.9	[75]
	α-Pinene	$C_{10}H_{16}$	25.0	[74]	82.8	83.1	[79]
	β-Pinene	$C_{10}H_{16}$	22.0	[74]	88.5	80.6	[79]
Aromatics	Tetralin	$C_{10}H_{12}$	9.4	[77]	106.6	96.5	[83]
	n-butylbenzene	$C_{10}H_{14}$	12.0	[74]	103.6	104.4	[75]
	Toluene	C_7H_8	6.0	[77]	109.9	120.0	[81]
	Ethylbenzene	C_8H_{10}	6.3	[77]	109.7	107.4	[75]
	m-xylene	C_8H_{10}	7.0	[77]	109.0	117.5	[75]
	o-xylene	C_8H_{10}	8.3	[77]	107.8	105.4	[15]
	p-xylene	C_8H_{10}	6.2	[77]	109.7	116.4	[75]
	Indan	C_9H_{10}	8.6	[77]	107.5	103.5	[75]
	1,2,3-trimethylbenzene	C_9H_{12}	10.1	[77]	105.9	105.3	[75]
	1,2,4-trimethylbenzene	C_9H_{12}	8.9	[77]	107.2	120.0	[53]
	1,3,5-trimethylbenzene	C_9H_{12}	8.0	[77]	108.1	> 120.0	[75]
Alcohols	Methanol	CH_4O	6.1	Measurement	109.8	122.0	[83]
	Ethanol	C_2H_6O	8.0	Measurement	108.1	109.0	[84]
	Propan-1-ol	C_3H_8O	8.2	Measurement	107.9	104.0	[85]
	Butan-2-ol	$C_4H_{10}O$	8.1	Measurement	108.0	105.0	[85]
	iso-butanol	$C_4H_{10}O$	8.5	[86]	107.6	105.0	[85]
	n-butanol	$C_4H_{10}O$	11.7	Measurement	104.0	98.0	[85]
	2-methylbutan-2-ol	$C_5H_{12}O$	12.1	[60]	103.5	97.0	[83]
	iso-pentanol	$C_5H_{12}O$	12.8	Measurement	102.6	98.8	[83]
	t-butanol	$C_4H_{10}O$	8.1	Measurement	108.0	107.0	[87]

Continued on next page

Table S6: (continued) Predicted RON from DCN obtained from literature and experiments in present work compared to nominal RON

	Fuel/Mixture	Formula	DCN	DCN reference	$RON_{predicted}$	RON	RON reference
Pyran	Tetrahydropyran	$C_5H_{10}O$	38.2	[60]	51.5	52.2	[79]
Ether	Methyl *tert*-butyl ether	$C_5H_{12}O$	8.5	[88]	107.6	118.0	[83]
Furans	2-methylfuran	C_5H_6O	9.1	[60]	106.9	100.7	[89]
	2,5-dimethylfuran	C_6H_8O	10.9	[90]	105.0	119.0	[91]
	2-methyltetrahydrofuran	$C_5H_{10}O$	21.3	[60]	89.7	88.2	[89]

[1] CN or DCN measured with unknown method
[2] Trans isomer of 3-octene
[3] RON of 3-octene, unknown which isomers were measured

Table S7: Predicted RON from DCN obtained from literature and experiments in present work compared to nominal RON

	Fuel/Mixture	Formula	DCN	DCN reference	$RON_{predicted}$	RON	RON reference
n-paraffins	*n*-hexane	C_6H_{14}	47.9	[74]	22.0	24.8	[75]
	n-hexane*	C_6H_{14}	50.0	[92]	14.9	24.8	[75]
	n-heptane	C_7H_{16}	53.8	[24]	1.3	0.0	[6]
	n-heptane*	C_7H_{16}	53.8	[74]	1.3	0.0	[6]
	n-heptane*	C_7H_{16}	53.0	[92]	4.2	0.0	[6]
	n-heptane*	C_7H_{16}	53.7	[93]	1.7	0.0	[6]
	n-heptane*	C_7H_{16}	53.8	[2]	1.3	0.0	[6]
	n-decane	$C_{10}H_{22}$	65.5	[74]	< 0.0	< 0.0	[76]
	n-decane*	$C_{10}H_{22}$	67.2	[94]	< 0.0	< 0.0	[76]
	n-dodecane	$C_{12}H_{26}$	72.9	[74]	< 0.0	< 0.0	[76]
	n-dodecane*	$C_{12}H_{26}$	74.0	[92]	< 0.0	< 0.0	[76]
iso-paraffins	2-methylbutane	C_5H_{12}	25.8	[77]	81.2	92.3	[75]
	2-methylbutane*	C_5H_{12}	24.0	[60]	84.7	92.3	[75]
	2-methylhexane	C_7H_{16}	43.5	[74]	36.0	42.4	[75]
	2-methylhexane*	C_7H_{16}	43.5	[95]	36.0	42.4	[75]

Continued on next page

Table S7: (continued) Predicted RON from DCN obtained from literature and experiments in present work compared to nominal RON

	Fuel/Mixture	Formula	DCN	DCN reference	$RON_{predicted}$	RON	RON reference
	2,3-dimethylpentane	C_7H_{16}	21.7	[77]	89.0	91.1	[75]
	2,3-dimethylpentane*	C_7H_{16}	22.0	[74]	88.5	91.1	[75]
	2,4-dimethylpentane	C_7H_{16}	28.2	[77]	76.2	83.1	[75]
	2,4-dimethylpentane*	C_7H_{16}	28.6	[45]	75.3	83.1	[75]
	2,4-dimethylpentane*	C_7H_{16}	28.7	[74]	75.0	83.1	[75]
	2-methylheptane	C_8H_{18}	47.0	[78]	24.9	21.7	[75]
	2-methylheptane*	C_8H_{18}	52.6	[74]	5.7	21.7	[75]
	2,2,4-trimethylpentane	C_8H_{18}	17.4	[24]	96.2	100.0	[6]
	2,2,4-trimethylpentane*	C_8H_{18}	17.2	[74]	96.5	100.0	[6]
Cycloalkanes	Methylcyclopentane	C_6H_{12}	17.2	[74]	96.5	91.3	[75]
	Methylcyclohexane*	C_7H_{14}	24.4	[74]	84.0	74.8	[82]
	Methylcyclohexane*	C_7H_{14}	22.0	[96]	88.5	74.8	[82]
	1,2,4-trimethylcyclohexane	C_9H_{18}	24.4	[60]	84.0	72.9	[83]
	1,2,4-trimethylcyclohexane*	C_9H_{18}	30.5	[83]	71.0	72.9	[83]

Continued on next page

Table S7: (continued) Predicted RON from DCN obtained from literature and experiments in present work compared to nominal RON

	Fuel/Mixture	Formula	DCN	DCN reference	$RON_{predicted}$	RON	RON reference
Cycloalkenes	α-Pinene	$C_{10}H_{16}$	25.0	[74]	82.8	83.1	[79]
	α-Pinene*	$C_{10}H_{16}$	18.9	[60]	93.8	83.1	[79]
	β-Pinene	$C_{10}H_{16}$	22.0	[74]	88.5	80.6	[79]
	β-Pinene*	$C_{10}H_{16}$	20.5	[60]	91.1	80.6	[79]
Aromatics	Tetralin	$C_{10}H_{12}$	9.4	[77]	106.6	96.5	[83]
	Tetralin*	$C_{10}H_{12}$	8.9	[74]	107.2	96.5	[83]
	Tetralin*	$C_{10}H_{12}$	21.3	[96]	89.7	96.5	[83]
	n-butylbenzene	$C_{10}H_{14}$	12.0	[74]	103.6	104.4	[75]
	n-butylbenzene*	$C_{10}H_{14}$	12.9	[60]	102.5	104.4	[75]
	1,2,4-trimethylbenzene	C_9H_{12}	8.9	[77]	107.2	120.0	[53]
	1,2,4-trimethylbenzene*	C_9H_{12}	8.9	[74]	107.2	120.0	[53]
Alcohols	Butan-2-ol	$C_4H_{10}O$	8.1	Measurement	108.0	105.0	[85]
	Butan-2-ol*	$C_4H_{10}O$	8.5	[86]	107.6	105.0	[85]
	n-butanol	$C_4H_{10}O$	11.7	Measurement	104.0	98.0	[85]
	n-butanol*	$C_4H_{10}O$	12.0	[86]	103.6	98.0	[85]
	iso-pentanol	$C_5H_{12}O$	12.8	Measurement	102.6	98.8	[83]
	iso-pentanol*	$C_5H_{12}O$	18.4	[74]	94.6	98.8	[83]
	iso-pentanol*	$C_5H_{12}O$	13.1	[60]	102.3	98.8	[83]

Table S8: Predicted RON from DCN obtained from literature with no supporting nominal RON

	Fuel/Mixture	Formula	DCN	DCN reference	$RON_{predicted}$
n-paraffins	*n*-hexadecane	$C_{16}H_{34}$	100.5	[74]	< 0.0
	n-hexadecane	$C_{16}H_{34}$	98.5	[60]	< 0.0
iso-paraffins	2,6-dimethyloctane	$C_{10}H_{22}$	51.7	[74]	8.9
	Farnesane (2,6,10-trimethyldodecane)	$C_{15}H_{32}$	58.0	[97]	< 0.0
	Farnesane (2,6,10-trimethyldodecane)	$C_{15}H_{32}$	59.1	[98]	< 0.0
	2,2,4,6,8,8-heptamethylnonane	$C_{16}H_{34}$	15.1	[74]	99.6
	2,2,4,6,8,8-heptamethylnonane	$C_{16}H_{34}$	14.2	[94]	100.8
	2,2,4,6,8,8-heptamethylnonane	$C_{16}H_{34}$	14.2	[60]	100.8
	2-methylheptadecane	$C_{18}H_{38}$	91.0	[74]	< 0.0
	2-methyloctadecane	$C_{19}H_{40}$	104.4	[74]	< 0.0
Olefins	1,9-decadiene	$C_{10}H_{18}$	41.0	[74]	43.5
	1-decene	$C_{10}H_{20}$	49.1	[74]	17.9
	1-dodecene	$C_{12}H_{24}$	56.8	[74]	< 0.0
	Bisabolene	$C_{15}H_{24}$	32.2	[74]	67.0
	1-hexadecene	$C_{16}H_{32}$	75.9	[74]	< 0.0
Alkynes	1-heptyne	C_7H_{12}	22.0	[74]	88.5
Cycloparaffins	*cis*-decalin	$C_{10}H_{18}$	41.6	[96]	41.8
	cis-decalin	$C_{10}H_{18}$	39.4	[74]	48.1
	trans-decalin	$C_{10}H_{18}$	32.0	[96]	67.5
	trans-decalin	$C_{10}H_{18}$	31.8	[74]	67.9
	n-butylcyclohexane	$C_{10}H_{20}$	47.6	[74]	23.0
	n-butylcyclohexane	$C_{10}H_{20}$	48.0	[78]	21.6
	Perhydro-phenanthrene	$C_{14}H_{24}$	38.8	[74]	49.8
Cycloolefins	1,5-cyclooctadiene	C_8H_{12}	25.7	[60]	81.4
	Limonene	$C_{10}H_{16}$	18.9	[60]	93.8
	γ-terpinene	$C_{10}H_{16}$	20.3	[60]	91.5
Aromatics	1,3,5-triethylbenzene	$C_{12}H_{18}$	7.6	[77]	108.5

Continued on next page

Table S8: (continued) Predicted RON from DCN obtained from literature with no supporting nominal RON

	Fuel/Mixture	Formula	DCN	DCN reference	$RON_{predicted}$
	1,3,5-triisopropylbenzene	$C_{15}H_{24}$	2.8	[74]	112.4
Aromatic oxygenates	Anisole	C_7H_8O	5.9	Measurement	110.0
	Benzyl alcohol	C_7H_8O	7.2	Measurement	108.8
	2-phenylethanol	$C_8H_{10}O$	6.9	Measurement	109.1
	1,2-dimethoxybenzene	$C_8H_{10}O_2$	9.8	[60]	106.2
	4-methoxybenzaldehyde	$C_8H_8O_2$	25.8	[60]	81.2
	Benzaldehyde dimethyl acetal	$C_9H_{12}O_2$	10.4	[60]	105.5
	α-methyl-*trans*-cinnamaldehyde	$C_{10}H_{10}O$	19.1	[60]	93.5
	Dibenzylether	$C_{14}H_{14}O$	8.1	[60]	108.0
Alcohols	Cyclopentanol	$C_5H_{10}O$	9.8	[60]	106.2
	Cyclohexanol	$C_6H_{12}O$	16.3	[60]	97.8
	1-heptanol	$C_7H_{16}O$	29.0	[74]	74.4
	3-octanol	$C_8H_{18}O$	25.1	[74]	82.6
	2-ethyl-1-hexanol	$C_8H_{18}O$	23.5	[74]	85.7
	1-octanol	$C_8H_{18}O$	33.7	[74]	63.3
	1-octanol	$C_8H_{18}O$	33.9	[60]	62.8
	2-nonanol	$C_9H_{20}O$	39.6	[74]	47.6
	Geraniol	$C_{10}H_{18}O$	16.5	[60]	97.5
	Linalool	$C_{10}H_{18}O$	12.9	[60]	102.5
	β-citronellol	$C_{10}H_{20}O$	25.6	[74]	81.6
	3,7-dimethyl-1-octanol	$C_{10}H_{22}O$	29.3	[74]	73.7
	Nerolidol	$C_{15}H_{26}O$	19.2	[60]	93.3
Ethers	Diethoxymethane	$C_3H_8O_2$	57.3	[60]	< 0.0
	1,2-dimethoxyethane	$C_4H_{10}O_2$	81.0	[60]	< 0.0
	2,2-dimethoxypropane	$C_5H_{12}O_2$	31.3	[60]	69.1
	3,4-dihydro-2H-pyran	C_5H_8O	23.9	[60]	84.9
	Cyclopentyl methyl ether	$C_6H_{12}O$	47.3	[60]	24.0
	Diisopropyl ether	$C_6H_{14}O$	23.6	[60]	85.5
	Acetaldehyde diethyl acetal	$C_6H_{14}O_2$	54.1	[60]	0.2
	Diethylene glycol dimethyl ether	$C_6H_{14}O_3$	315.7	[60]	< 0.0
	hexylmethyl ether	$C_7H_{16}O$	99.8	[74]	< 0.0
	1-butoxy-2-propanol	$C_7H_{16}O_2$	36.1	[74]	57.1
	Dipropylene glycol monomethyl ether	$C_7H_{16}O_3$	43.9	[74]	34.8

Continued on next page

Table S8: (continued) Predicted RON from DCN obtained from literature with no supporting nominal RON

	Fuel/Mixture	Formula	DCN	DCN reference	$RON_{predicted}$
	Triethylene glycol monomethyl ether	$C_7H_{16}O_4$	80.7	[74]	< 0.0
	Diisobutyl ether	$C_8H_{18}O$	59.7	[74]	< 0.0
	Dibutyl ether	$C_8H_{18}O$	115.4	[60]	< 0.0
	Eucalyptol	$C_{10}H_{18}O$	18.8	[60]	94.0
	Diisoamyl ether	$C_{10}H_{22}O$	96.3	[74]	< 0.0
	Tripropylene glycol monomethylether	$C_{10}H_{22}O_4$	81.3	[74]	< 0.0
	Rose oxide	$C_{10}H_8O$	30.0	[74]	72.1
	1,4-cyclohexanedimethanol divinyl ether	$C_{12}H_{20}O_2$	61.1	[60]	< 0.0
	Dodecyl vinyl ether	$C_{14}H_{28}O_2$	101.7	[60]	< 0.0
Furans	Tetrahydrofuran	C_4H_8O	21.9	[60]	88.7
	Furfural	$C_5H_4O_2$	13.9	[60]	101.2
	2-ethyltetrahydrofuran	$C_6H_{12}O$	28.1	[90]	76.4
	2-ethylfuran	C_6H_8O	10.2	[90]	105.7
	Tetrahydrofurfurylacetate	$C_7H_{12}O_3$	18.2	[60]	94.9
	2-butylfuran	$C_8H_{12}O$	13.1	[90]	102.3
	2-butyltetrahydrofuran	$C_8H_{16}O$	45.5	[90]	29.8
Aldehydes	Butanal	C_4H_8O	41.1	[60]	43.2
	isobutyraldehyde	C_4H_8O	21.1	[60]	90.1
	Pentanal	$C_5H_{10}O$	62.2	[60]	< 0.0
	Hexanal	$C_6H_{12}O$	75.2	[60]	< 0.0
	3-cyclohexene-1-carboxaldehyde	$C_7H_{10}O$	28.1	[60]	76.4
	Octanal	$C_8H_{16}O$	80.5	[74]	< 0.0
	Octanal	$C_8H_{16}O$	102.5	[60]	< 0.0
Ketones	3-pentanone	$C_5H_{10}O$	19.5	[60]	92.8
	2-heptanone	$C_6H_{10}O$	30.0	[74]	72.1
	Cyclohexanone	$C_6H_{10}O$	10.4	[60]	105.5
	4-methyl-2-pentanone	$C_6H_{12}O$	12.6	[60]	102.9
	Cycloheptanone	$C_7H_{12}O$	22.5	[60]	87.6
	2,4-dimethyl-3-pentanone	$C_7H_{14}O$	15.8	[60]	98.6
	3-octanone	$C_8H_{16}O$	36.0	[74]	57.4
	2-octanone	$C_8H_{16}O$	36.6	[60]	55.8
	3,3,5-trimethylcyclohexanone	$C_9H_{16}O$	11.9	[60]	103.8
	2-nonanone	$C_9H_{18}O$	46.1	[60]	27.9
	Menthone	$C_{10}H_{18}O$	20.6	[60]	91.0

Continued on next page

Table S8: (continued) Predicted RON from DCN obtained from literature with no supporting nominal RON

	Fuel/Mixture	Formula	DCN	DCN reference	$RON_{predicted}$
Esters	Methyl pentanoate	$C_6H_{12}O_2$	13.3	[86]	102.0
	Methyl sorbate	$C_7H_{10}O_2$	6.0	[74]	109.9
	Methyl caproate	$C_7H_{14}O_2$	23.9	[74]	84.9
	Ethyl pentanoate	$C_7H_{14}O_2$	18.6	[86]	94.3
	Methyl hexanoate	$C_7H_{14}O_2$	25.3	[60]	82.2
	Methyl heptanoate	$C_8H_{16}O_2$	34.2	[74]	62.0
	Butyl butanoate	$C_8H_{16}O_2$	17.8	[74]	95.6
	n-hexyl acetate	$C_8H_{16}O_2$	33.8	[74]	63.1
	Propyl pentanoate	$C_8H_{16}O_2$	20.7	[86]	90.8
	Hexyl acetate	$C_8H_{16}O_2$	32.2	[60]	67.0
	Ethyl hexanoate	$C_8H_{16}O_2$	27.5	[60]	77.6
	Butyl levulinate	$C_9H_{16}O_3$	14.4	[74]	100.5
	Butyl pentanoate	$C_9H_{18}O_2$	23.5	[86]	85.7
	Pentyl pentanoate	$C_{10}H_{20}O_2$	28.8	[74]	74.8
	Pentyl pentanoate	$C_{10}H_{20}O_2$	27.6	[86]	77.4
	Methyl-9-decenoate	$C_{11}H_{20}O_2$	38.3	[74]	51.2
	Methyl decanoate	$C_{11}H_{22}O_2$	52.7[2]	[74]	5.3
	Methyl decanoate	$C_{11}H_{22}O_2$	50.7	[74]	12.4
	Methyl decanoate	$C_{11}H_{22}O_2$	51.6	[99]	9.3
	Methyl decanoate	$C_{11}H_{22}O_2$	54.1	[94]	0.2
	Menthyl acetate	$C_{12}H_{22}O_2$	19.5	[60]	92.8
	Methyl laurate	$C_{13}H_{26}O_2$	66.7	[99]	< 0.0
	Methyl laurate	$C_{13}H_{26}O_2$	66.3	[74]	< 0.0
	Vinyl laurate	$C_{14}H_{26}O_2$	77.0	[60]	< 0.0
	Methyl tetradecanoate	$C_{15}H_{30}O_2$	75.8	[60]	< 0.0
	Methyl palmitate	$C_{17}H_{34}O_2$	85.9	[99]	< 0.0
	Methyl linolenate	$C_{19}H_{32}O_2$	37.0	[74]	54.7
	Methyl gamma linolenate	$C_{19}H_{32}O_2$	29.2	[100]	73.9
	Methyl alpha linolenate	$C_{19}H_{32}O_2$	22.7	[101]	87.2
	Methyl linoleate	$C_{19}H_{34}O_2$	43.9	[74]	34.8
	Methyl linoleate	$C_{19}H_{34}O_2$	38.2	[99]	51.5
	Methyl linolelaidate	$C_{19}H_{34}O_2$	43.0	[101]	37.6
	Methyl oleate	$C_{19}H_{36}O_2$	59.8	[74]	< 0.0
	Methyl oleate	$C_{19}H_{36}O_2$	56.6	[99]	< 0.0
	Methyl oleate	$C_{19}H_{36}O_2$	59.3	[57]	< 0.0

Continued on next page

Table S8: (continued) Predicted RON from DCN obtained from literature with no supporting nominal RON

	Fuel/Mixture	Formula	DCN	DCN reference	$RON_{predicted}$
Esters	Methyl petroselinate	$C_{19}H_{36}O_2$	58.6	[101]	< 0.0
	Methyl elaidate	$C_{19}H_{36}O_2$	57.2	[101]	< 0.0
	Methyl ricinoleate	$C_{19}H_{36}O_3$	37.4	[99]	53.7
	Methyl stearate	$C_{19}H_{38}O_2$	95.6	[74]	< 0.0
	Methyl asclepate	$C_{19}H_{38}O_2$	53.9	[101]	0.9
	Methyl-5(Z)8(Z)11(Z)14(Z)-eicosatetraenoate	$C_{21}H_{34}O_2$	29.6	[102]	73.0
	Methyl gondoate	$C_{21}H_{40}O_2$	73.2	[103]	< 0.0
	Methyl-4(Z),7(Z),10(Z),13(Z),16(Z),19(Z)-docosahexaenoate	$C_{23}H_{34}O_2$	24.4	[102]	84.0
	Methyl erucate	$C_{23}H_{44}O_2$	74.2	[103]	< 0.0

[1] Contaminants removed by treating with silica gel